



**Metamaterials,
Metasurfaces, and
Nanotechnology, and their
Applications to Antennas,
Sensors, and Cognitive Radar**



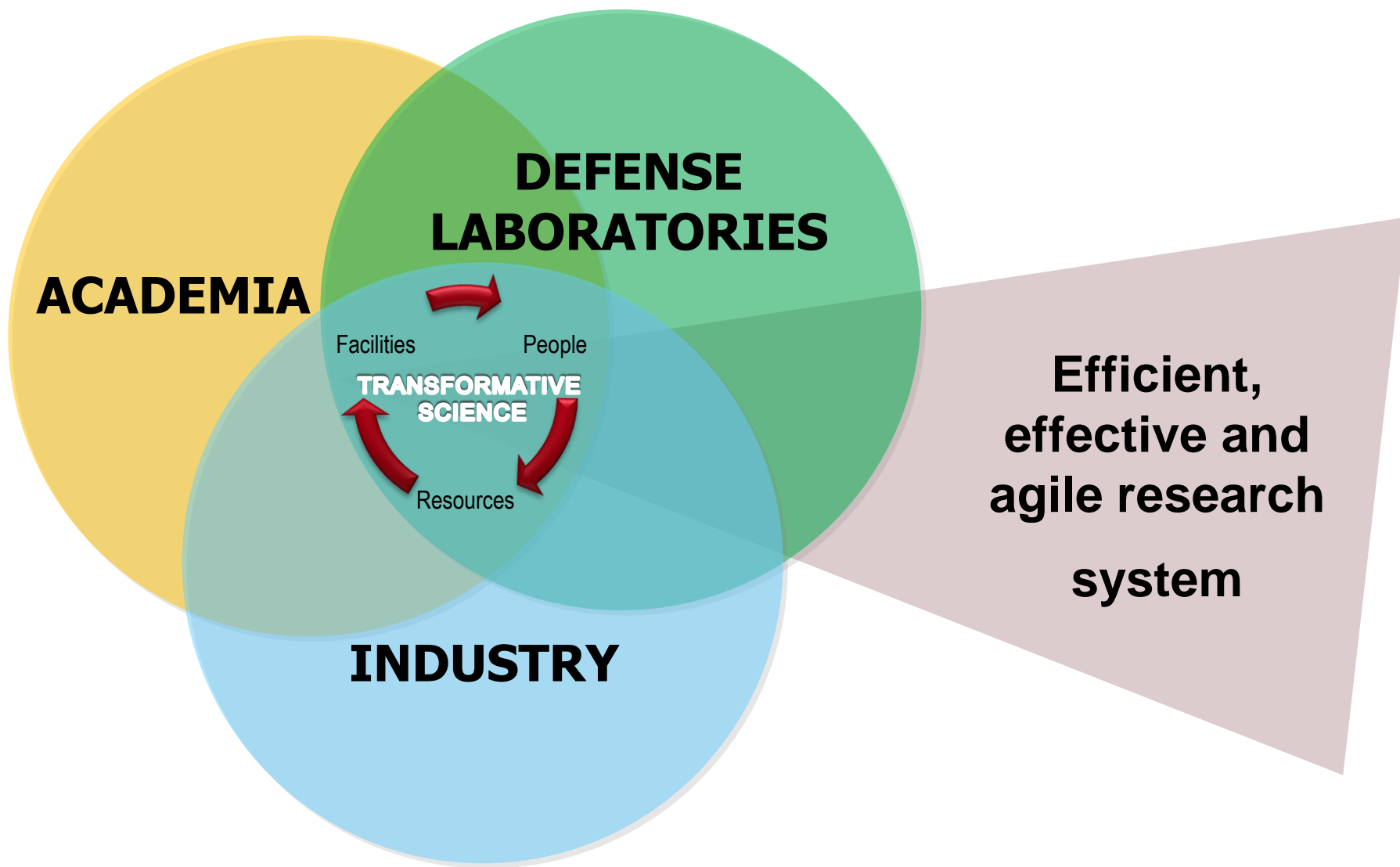
Amir I. Zaghloul

**ECE Department, Virginia Tech
and U.S. Army Research Laboratory, Adelphi, MD 20783**

**Presentation at Virginia Tech, Blacksburg
March 19, 2014**

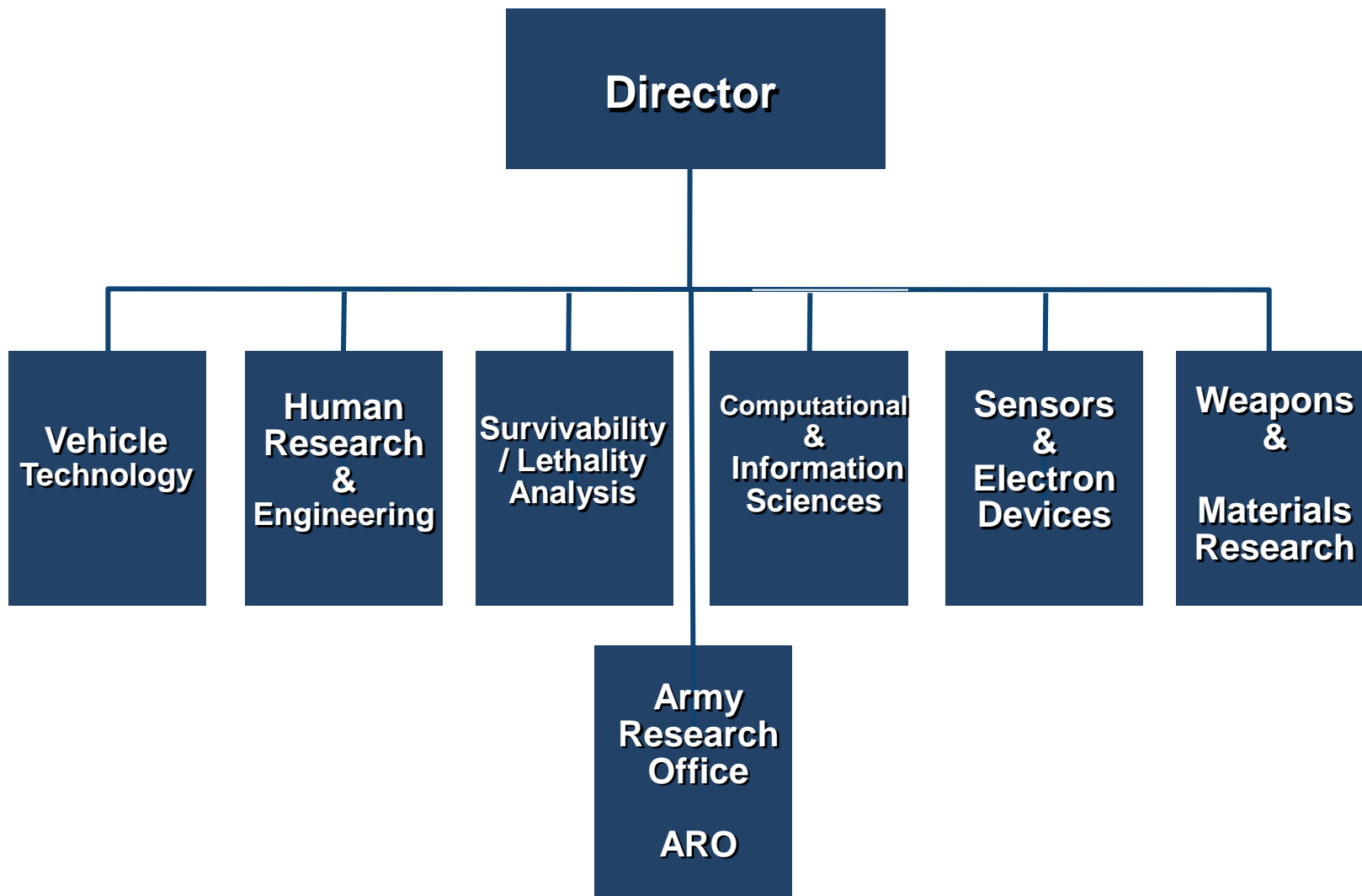


- **Introduction**
- **Metamaterials**
 - Negative Refractive Index
 - Periodic and Random Material
 - Application to Enhanced Dipole Antenna
 - Application to Rotman lens
- **Metasurfaces**
 - Electromagnetic Band-Gap Surfaces
 - Wideband EBG Surfaces
 - Adaptive and Active Reflection Phase Surfaces
 - Application to Spiral Antennas
 - Application to Cognitive Radar
- **Nanotechnology**
 - Carbon Nano-Tubes
 - CNT Patches
 - Application to Gas Sensors
 - Application to Polarization-Selective Patches
- **Conclusions**





- Campus-like environment with collaborative space
- Ready access for all partners including foreign nationals
- Expansion of academic programs & collaboration
- Access to world-renown facilities and resources
- Synergistic with MD and DC metro area entrepreneur community
 - Better focus of small business innovative research (SBIR) investments

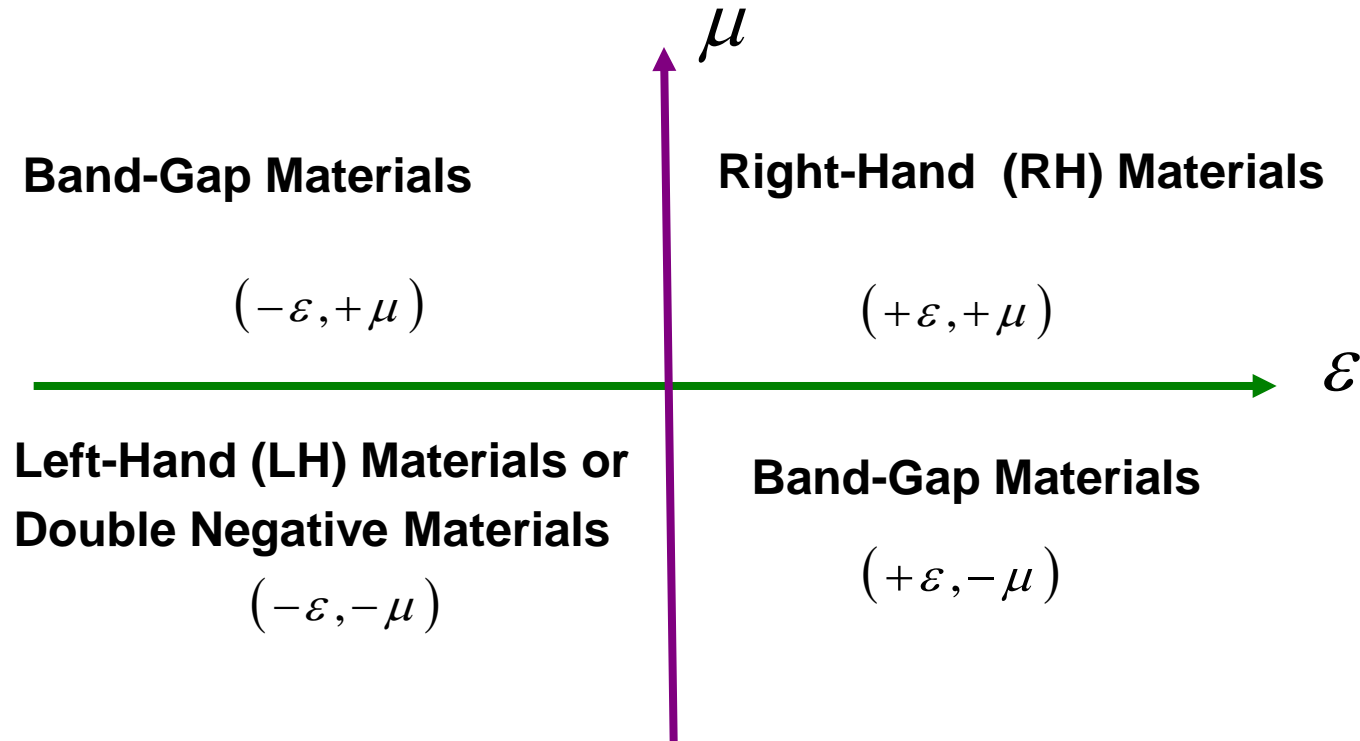




- **Introduction**
- **Metamaterials**
 - **Negative Refractive Index**
 - **Periodic and Random Material**
 - **Application to Enhanced Dipole Antenna**
 - **Application to Rotman Lens**
- **Metasurfaces**
 - **Electromagnetic Band-Gap Surfaces**
 - **Wideband EBG Surfaces**
 - **Adaptive and Active Reflection Phase Surfaces**
 - **Application to Spiral Antennas**
 - **Application to Cognitive Radar**
- **Nanotechnology**
 - **Carbon Nano-Tubes**
 - **CNT Patches**
 - **Application to Gas Sensors**
 - **Application to Polarization-Selective Patches**
- **Conclusions**



A Definition: A class of engineered materials that exhibit highly beneficial electromagnetic properties, which are not naturally occurring or common synthetic materials



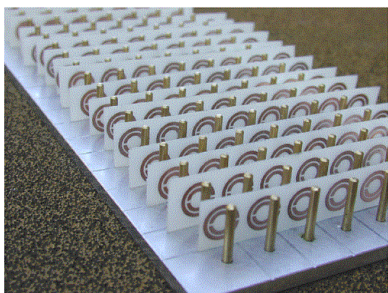
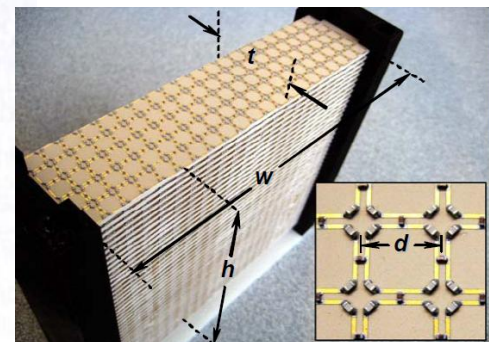
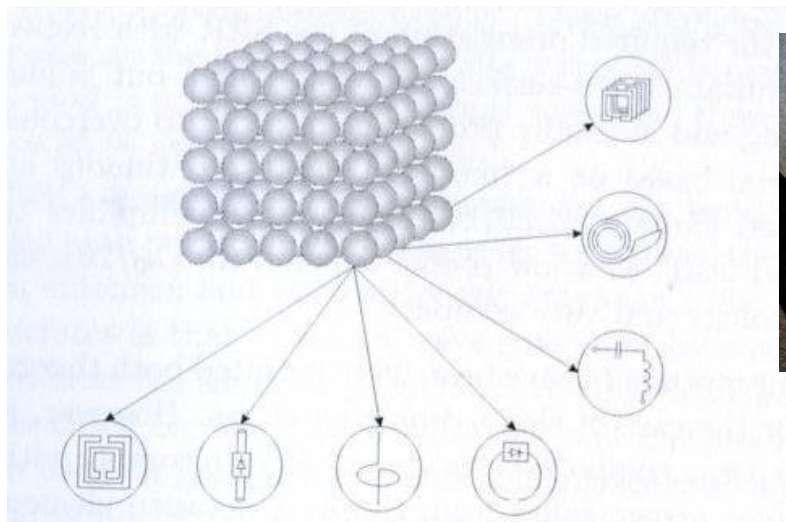


Some Specific Metamaterials Design Goals

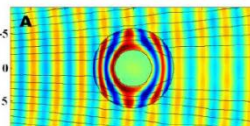
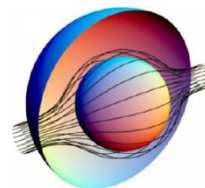
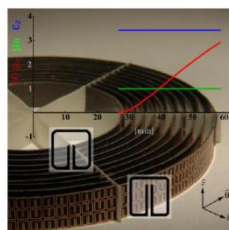


- **Metamaterials present themselves as an additional “tool set” for designing and enhancing antenna performance**
 - **Investigate metamaterial magnetic ground planes to reduce planar antenna sizes**
 - **Applicable to conformal platform applications**
 - **Investigate metamaterials to impedance match embedded antennas in platform thus improving bandwidth**
 - **Investigate metamaterials to reduce mutual coupling between antennas operating at different frequencies**
 - **Mitigate co-site interference**
 - **Improve array performance**

- Printed elements/circuits on dielectric material in a periodic structure



A split ring structure etched into copper circuit board plus copper wires to give negative μ and negative ϵ (courtesy David Smith and Shelly Schultz, UCSD).



Smith, et al., @ Duke Univ., 2006



Metamaterial and Metamaterial-Inspired Antennas

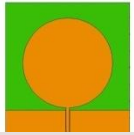


Metamaterial Antennas - ones made from ideal homogenized metamaterials where the behavior of the unit cells gives effective macroscopic parameters.

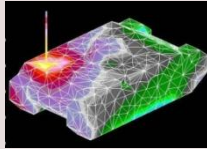
Metamaterial inspired - designs that are realized from understanding metamaterial concepts, but cannot be called metamaterials (e.g., an antenna constructed with one “unit cell.”) Often the designs are realized by a few metallic inclusions (e.g., split ring resonators,) but could have been realized using well-known traditional methods.



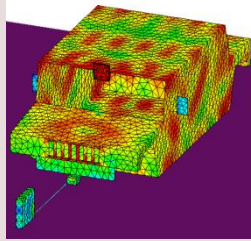
Army/ARL RF Metamaterials Research & Development



Metamaterials can be used to broadband (impedance match) antennas



Metamaterials can be used to mitigate "hot spots"

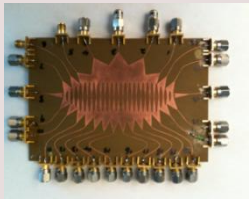


Metamaterials can integrate antennas into armor

Accurate analytical and numerical tool for periodic-metal-insert metamaterials

Random-metal-insert metamaterials for broadband applications

Analytical and numerical tools for general metamaterial configurations.



Duke Univ. Metamaterial Rotman lens



General Atomics/Metamaterial Belt Antenna for the Soldier

ARL Measures University of Michigan/CERDEC Metamaterial structure to validate performance enhancement.

ARL fabricates a class Of metamaterial at RF For optimization of antenna performance.

Victor Veselago Writes a theoretical Paper discussing the Implications of double Negative materials.

2000

2007

2008

2009

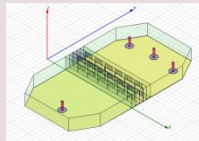
2010

2011

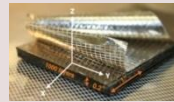
2012

2013....

ARL fabricates double negative test structures for proof of feasibility



ARL is contracting agent With MetaMaterials, Inc for Metaferrite antenna development



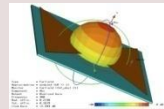
ARL field tests Metamaterial antennas On Army platforms

Prototype Antennas Fabricated and Measured



ARL develops Volumetric Randomly Oriented Unit Cells for Isotropic Performance

ARL identifies significant Modeling issues and defines needs for the MSME



1967

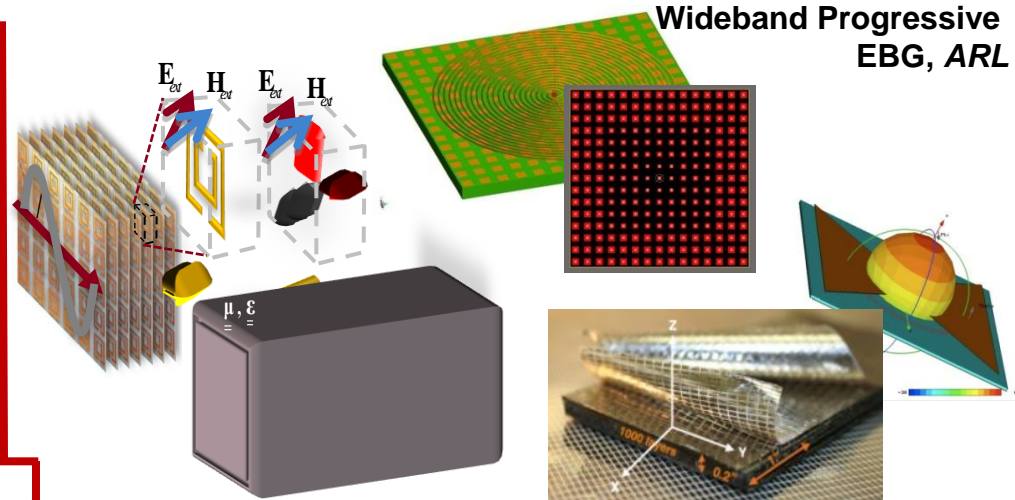


Metamaterial Antenna Work at the Army Research Laboratory



OBJECTIVES

- Investigate metamaterial structures for insertion in Army platforms to accomplish:
 - Size reduction, lower profile, and improved performance/higher gains of antennas
 - Wideband operation



Multilayer Metamaterial Analysis, *Univ. of Siena*, Metaferrite Surface, *Metamaterials, Inc Italy*

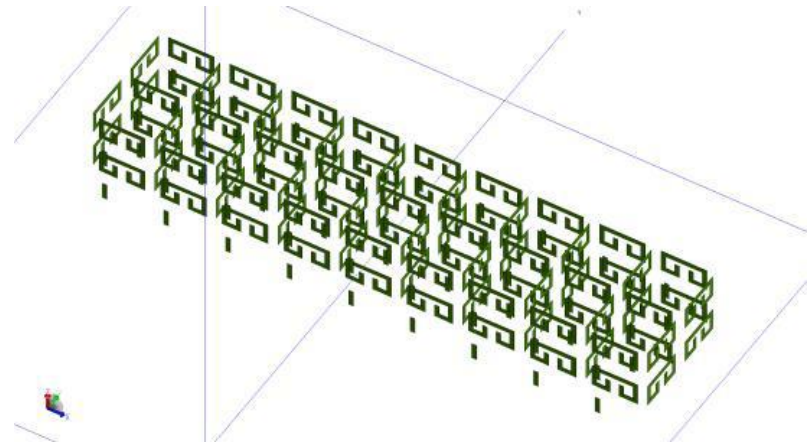
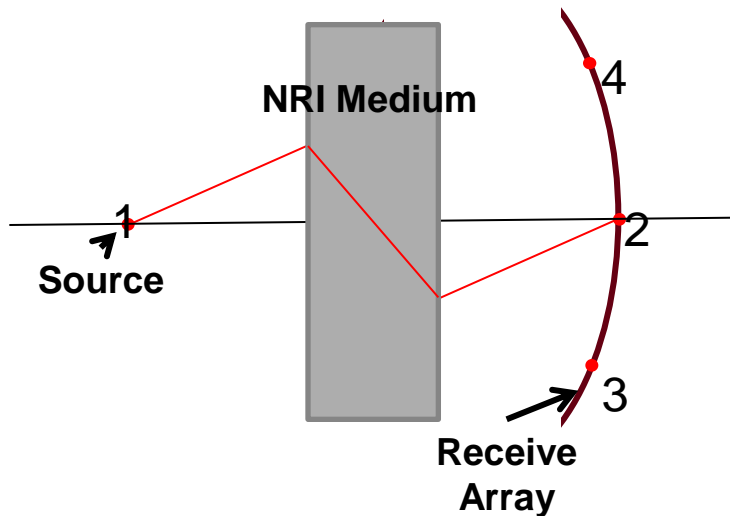
APPROACH

- Use negative refractive index materials for new optics with smaller overall dimensions
- Use random metamaterials for possible wideband operation and lower losses
- Use metaferrites with high permeability to reduce profile of planar antennas
- Develop generalized analytical tools to deduce the parameters of multilayer metamaterials
- Use progressive dimensions and stacked EBG surfaces for low profile antennas

ACCOMPLISHMENTS

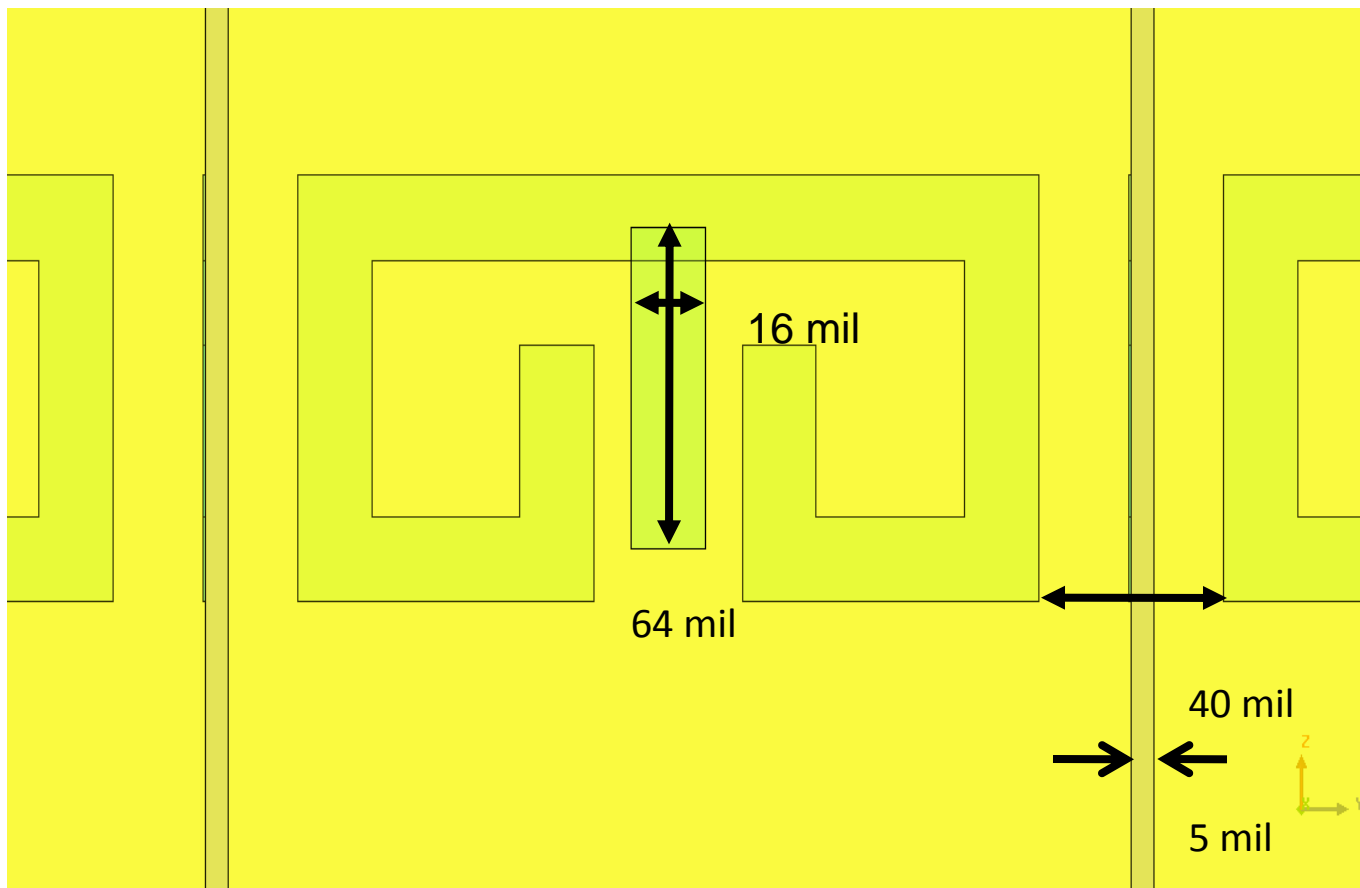
- Light-weight, thin metaferrite material was built and low-profile, wide bandwidth antenna was demonstrated
- Rigorous formulation of anisotropic multilayer metamaterial was used to calculate bulk constitutive parameters
- Wideband (>4:1 ratio) EBG surface was shown to improve the performance of broadband antennas, e.g. spiral antenna

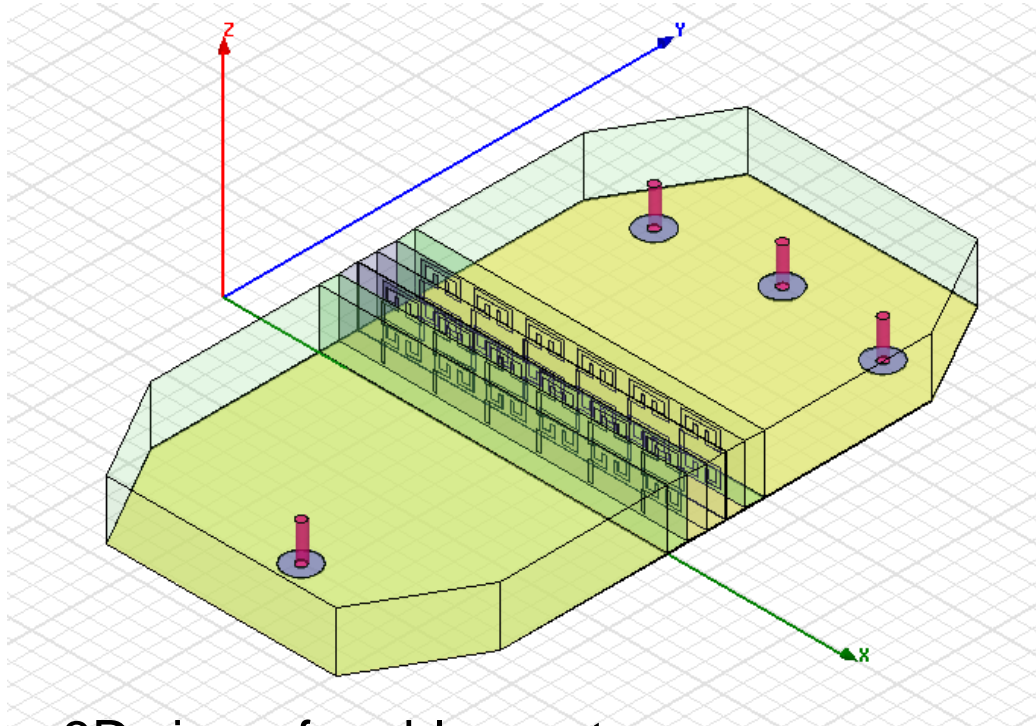
- Prove through simulation and measurements refractive focusing using NRI metamaterials
- Show near-isotropic NRI behavior in a Capacitively Loaded Loop plus Probe (CLL-P) slab



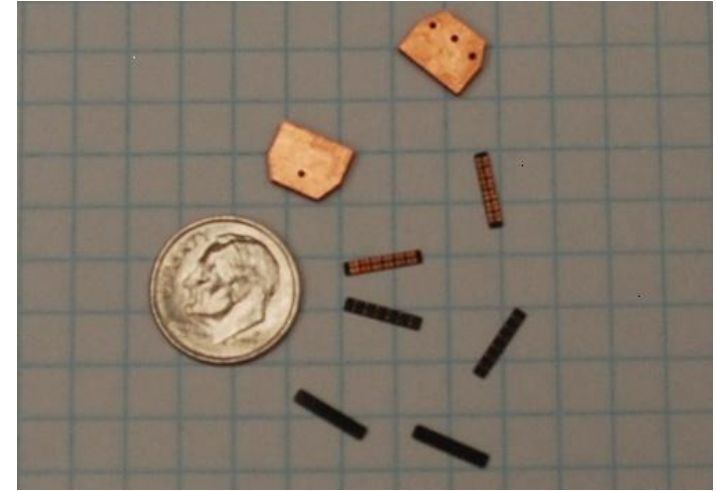


Unit Cell Details



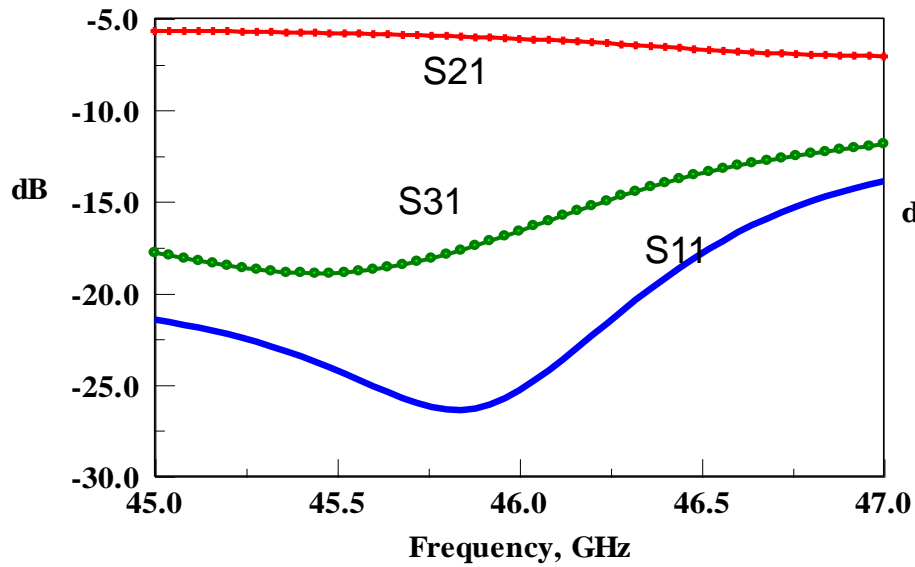


- 3D view of problem setup
- Height of dielectric 61 mil
- Dielectric constant 2.3
- Frequency range 45 – 47 GHz
- Wavelength at 46 GHz: 6.52 mm, 257 mil

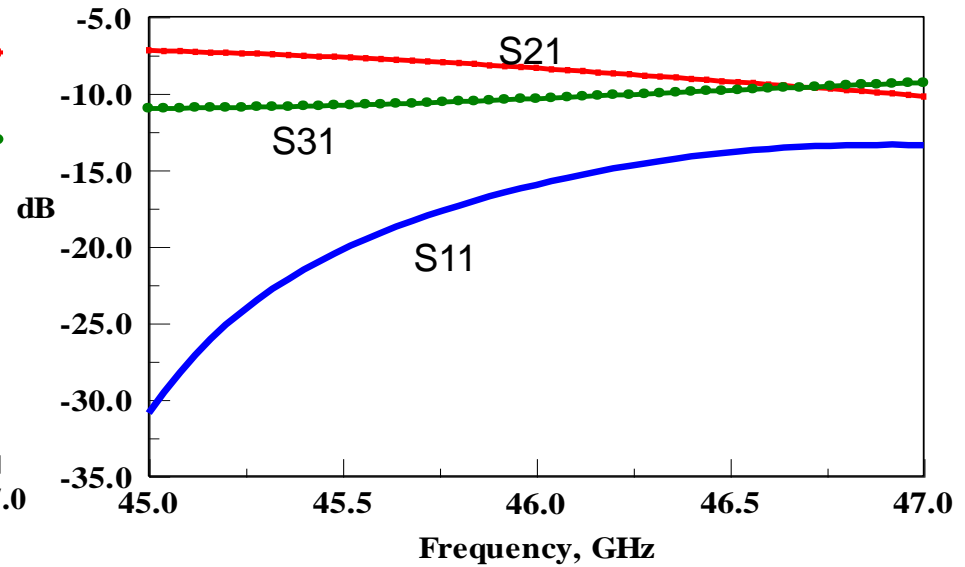




Refractive Focusing Using Negative-Refractive-Index Metamaterials



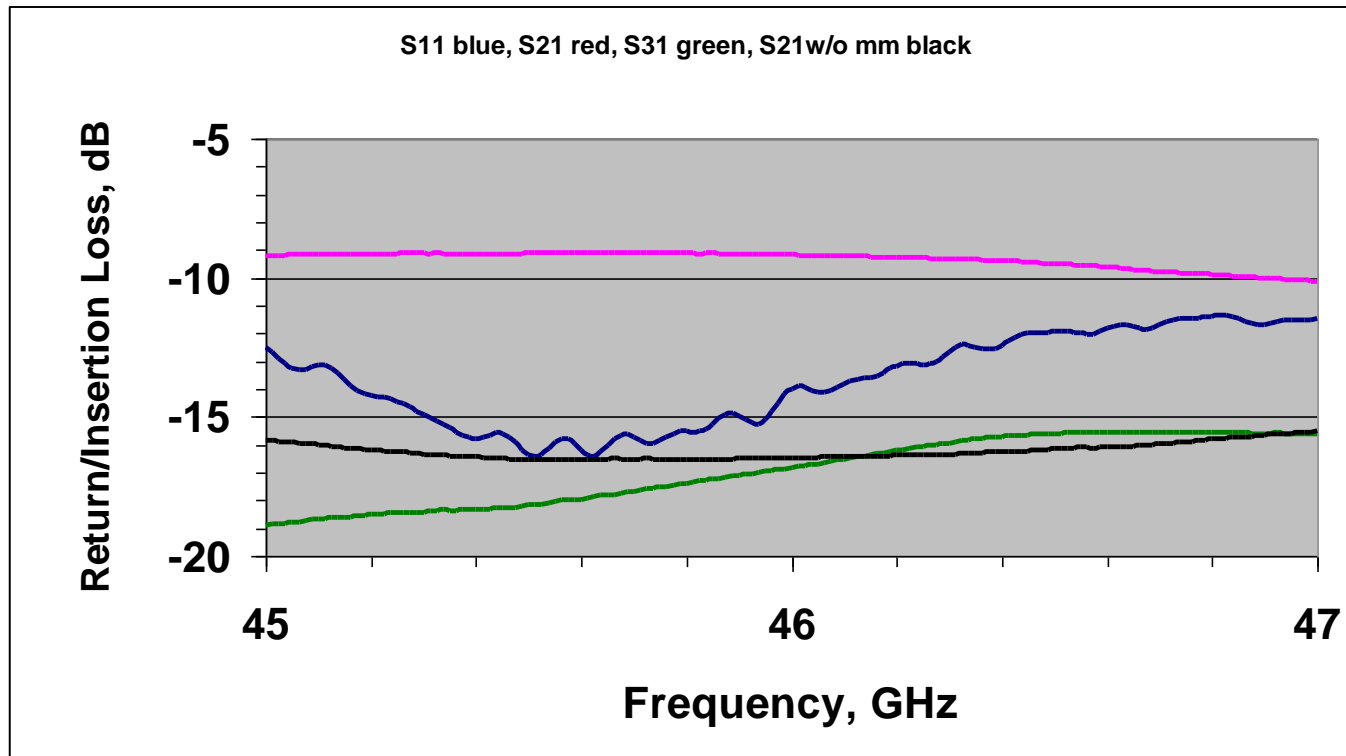
Simulated S-Parameters with Metamaterial



Simulated S-Parameters without Metamaterial

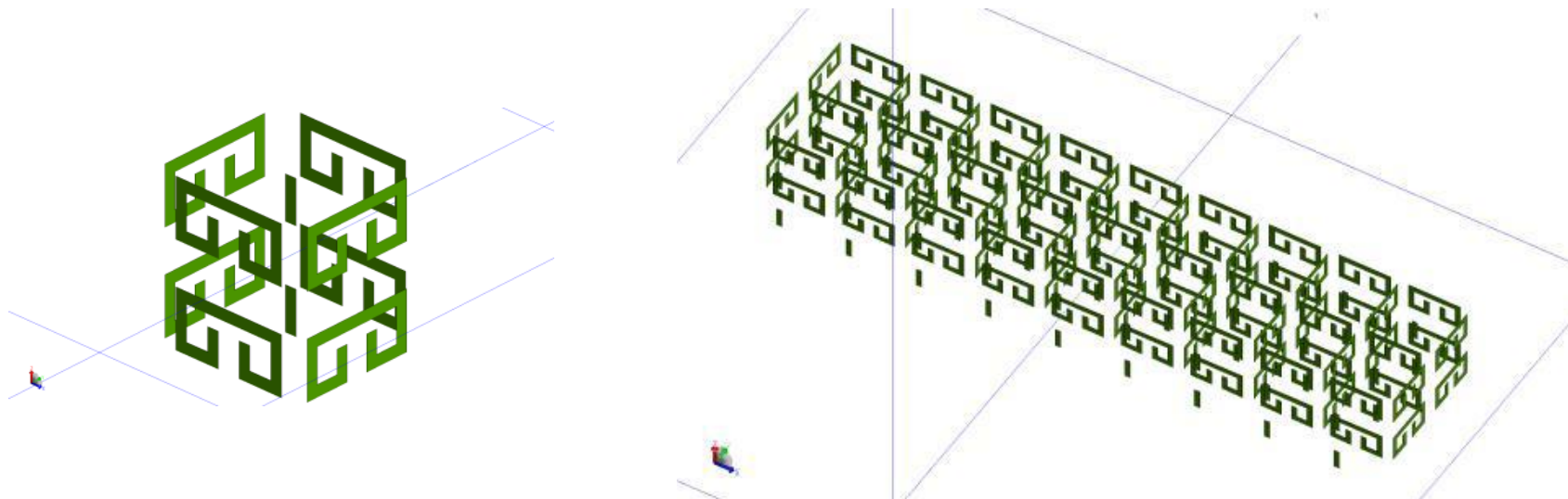


Refractive Focusing Using Negative-Refractive-Index Metamaterials

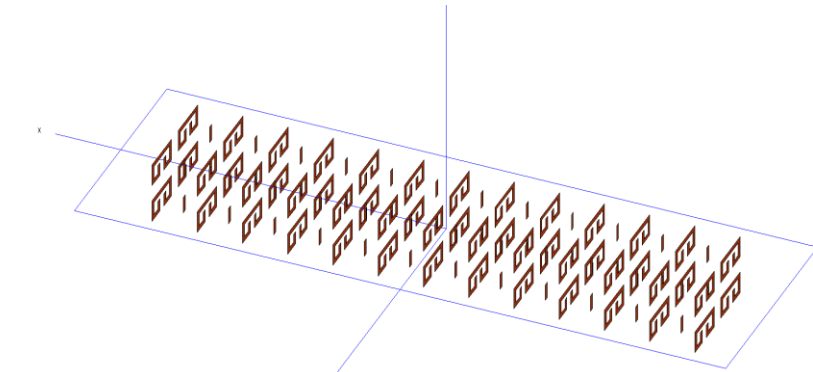


Measured S-Parameters

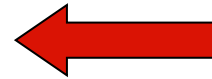
- S11 with metamaterial
- S21 with metamaterial
- S31 with metamaterial
- S21 without metamaterial



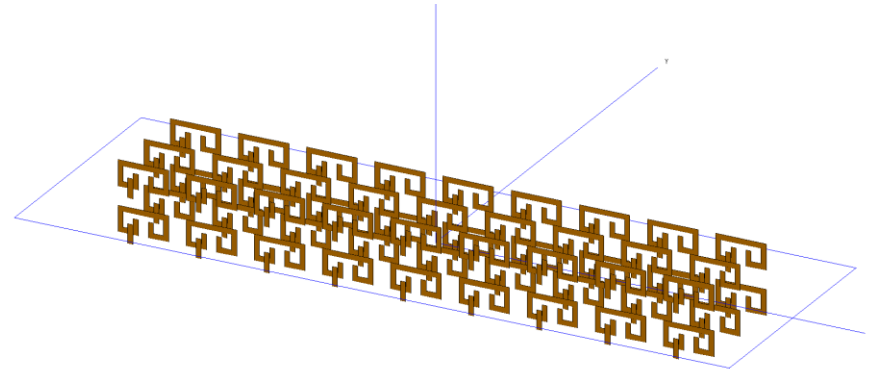
- Full-wave simulation of parallel slab
- Unit cell is a Capacitively Loaded Loop + Probe (CLL-P)
- Refractive index is calculated using Snell's Law and S-parameters
=> agreement
- Uniform negative refractive index at wide inclined angles => isotropic



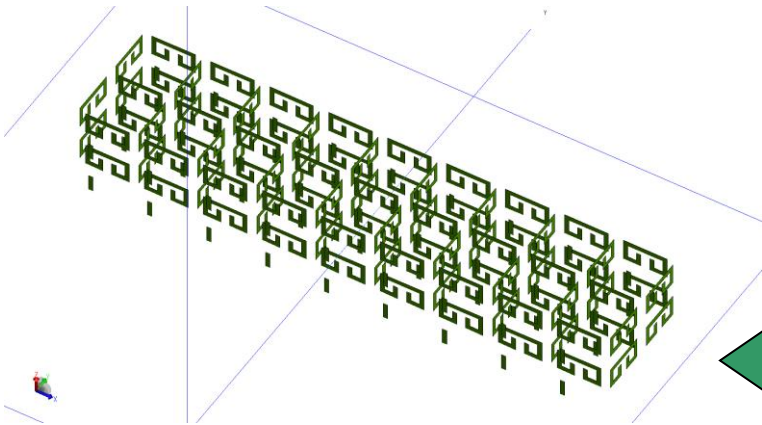
Vertical CLL-P Configuration: Couples to lateral component of magnetic field

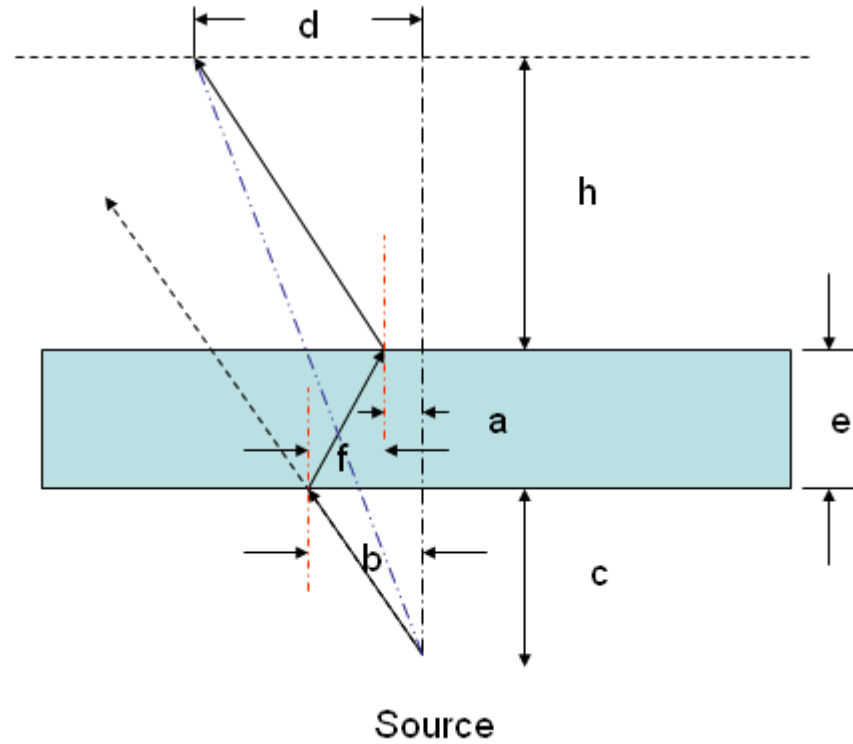


Parallel CLL-P Configuration: Couples to longitudinal component of magnetic field



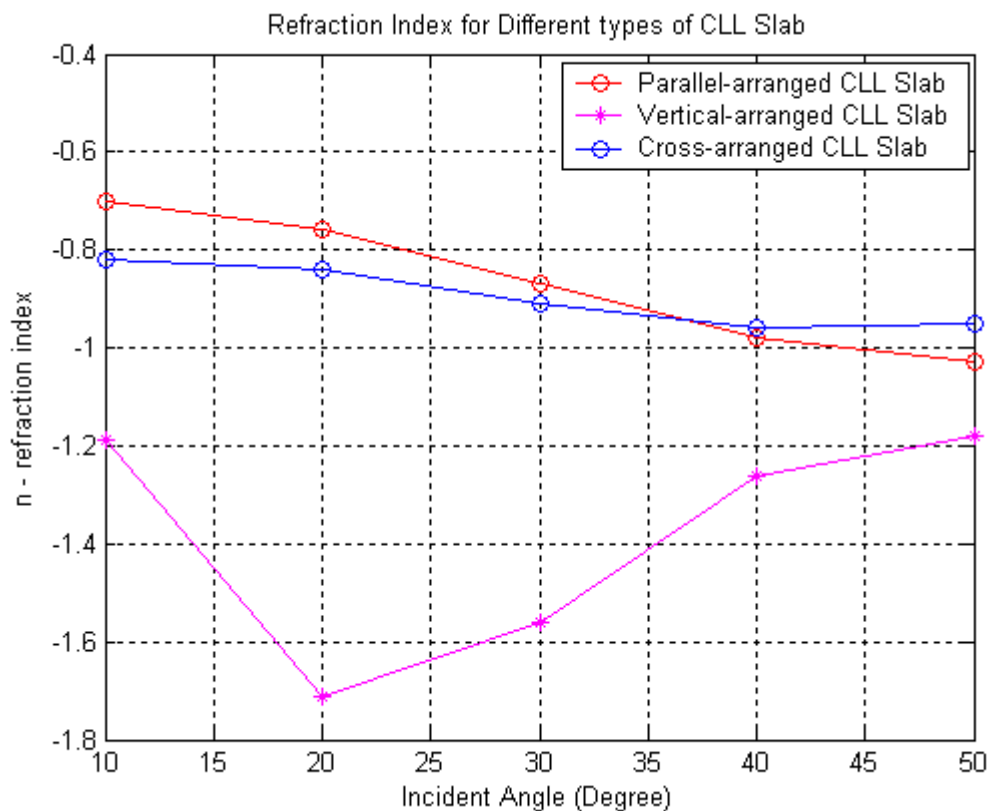
Cross CLL-P Configuration: Couples to both components of magnetic fields for isotropic characteristics



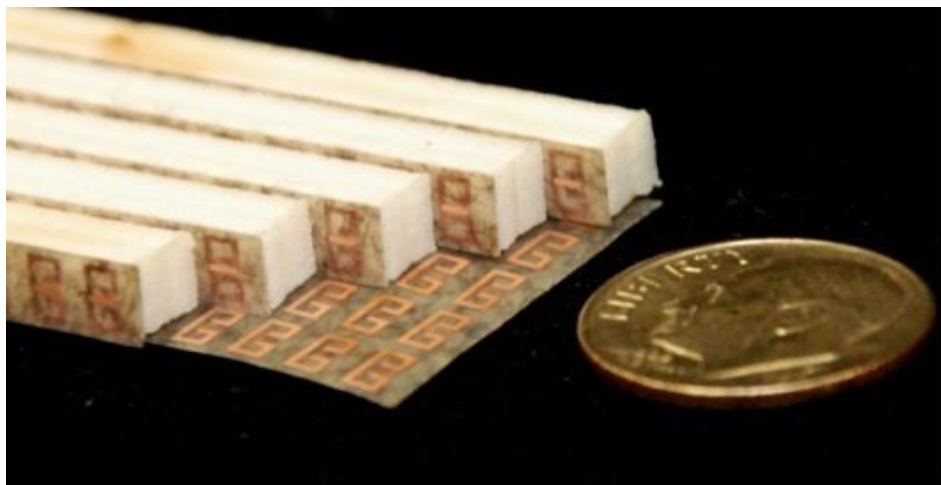




Comparison of the Refractive Index for Different Types of CLL Slabs



Isotropic negative refractive index in cross-arranged CLL slab

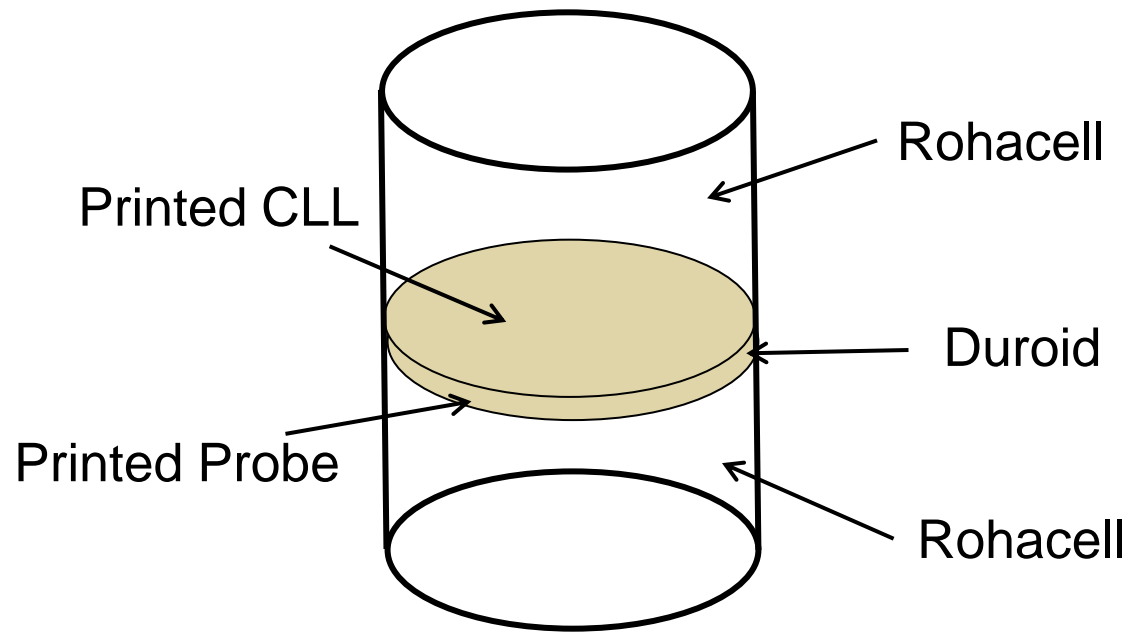


Periodic
metamaterial
configuration

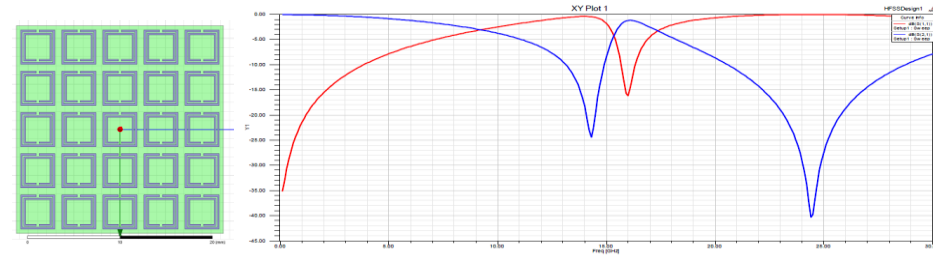


Random
metamaterial
configuration

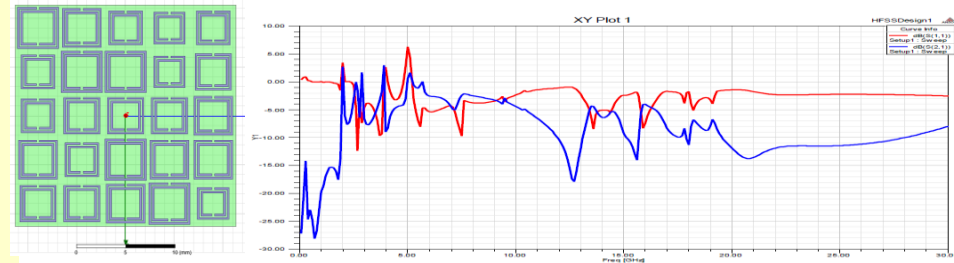




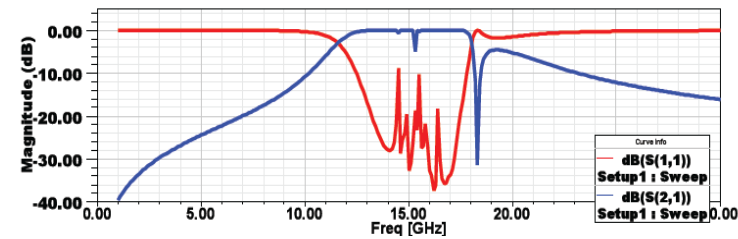
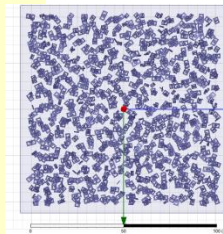
- Develop wideband control of metamaterial transmission and reflection properties as an alternative to adaptive narrowband tuning
- Application-specific metamaterials: band-pass, band-stop, reflection-enhanced surfaces
- Explore the characteristics of randomly oriented cells in metamaterials:
 - Broader transmission/reflection bandwidth
 - Applied to fabrication disorders in otherwise periodic metamaterials
 - Study orthogonal incidences and polarization properties



Periodic Lattice with Uniform Cells

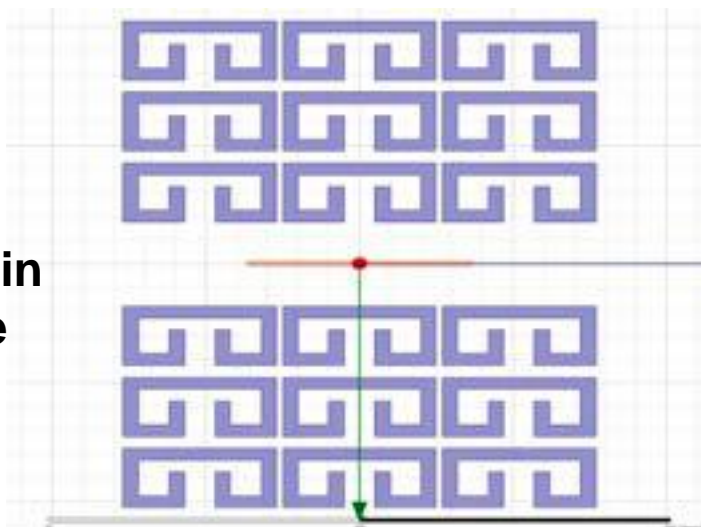


Periodic Lattice with Disordered Cells



Random Cells

Planar, 2-Fin Structure



12-Fin Structure

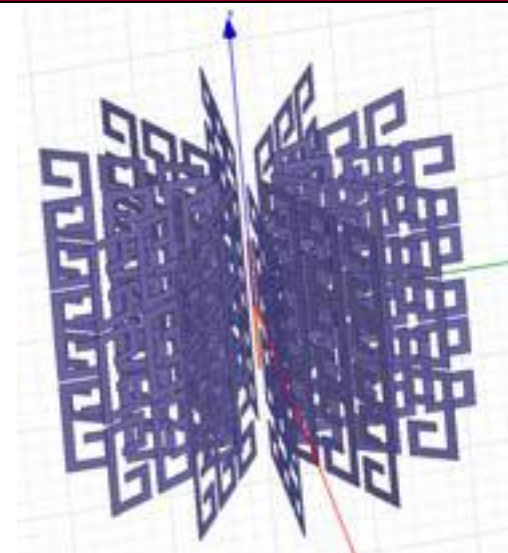
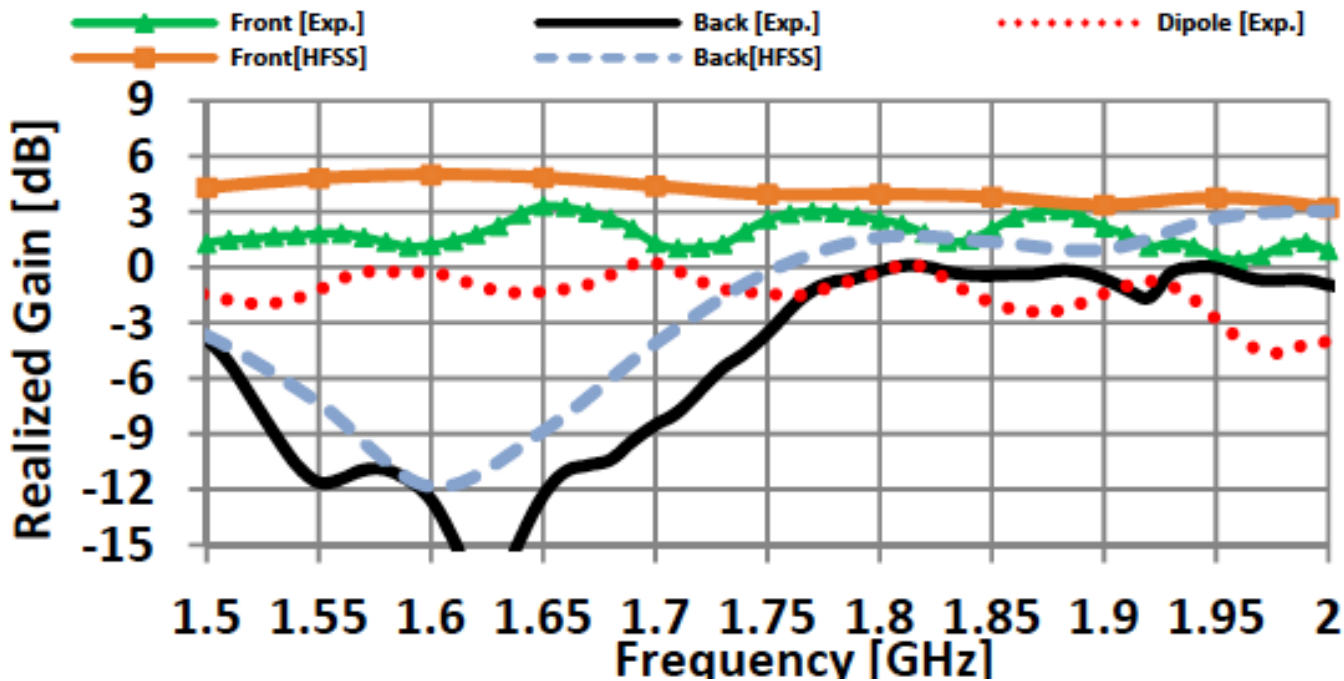
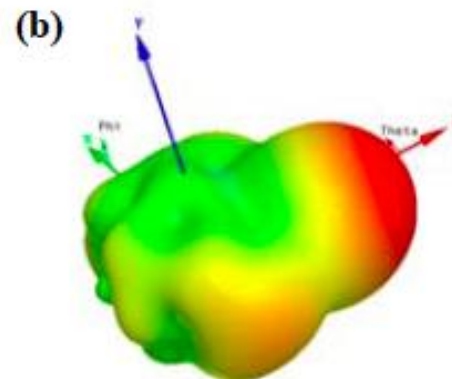
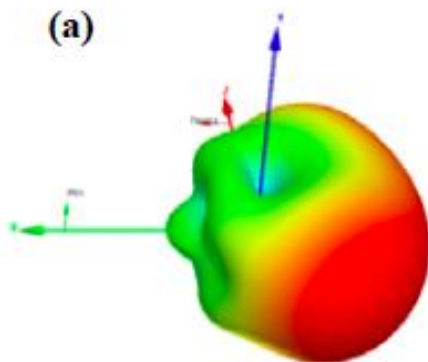


TABLE I. HFSS SIMULATION RESULTS FOR STRUCTURES BASED ON # OF CLL FINS.

# of CLL Fins	Max Gain (dB)	Gain Improvement (dB)	3-dB Beamwidth (degrees)	Frequency of Max Gain (GHz)	Front-to-Back Ratio (dB)
0	2.2	0	360°	15.3	0
2	5.4	3.2	165.1°	19.3	9.3
4	6.9	4.7	95.7°	19.7	3.2
8	7.8	5.7	88.9°	20.8	10.7
12	9.7	7.5	48.3°	20.5	12.4



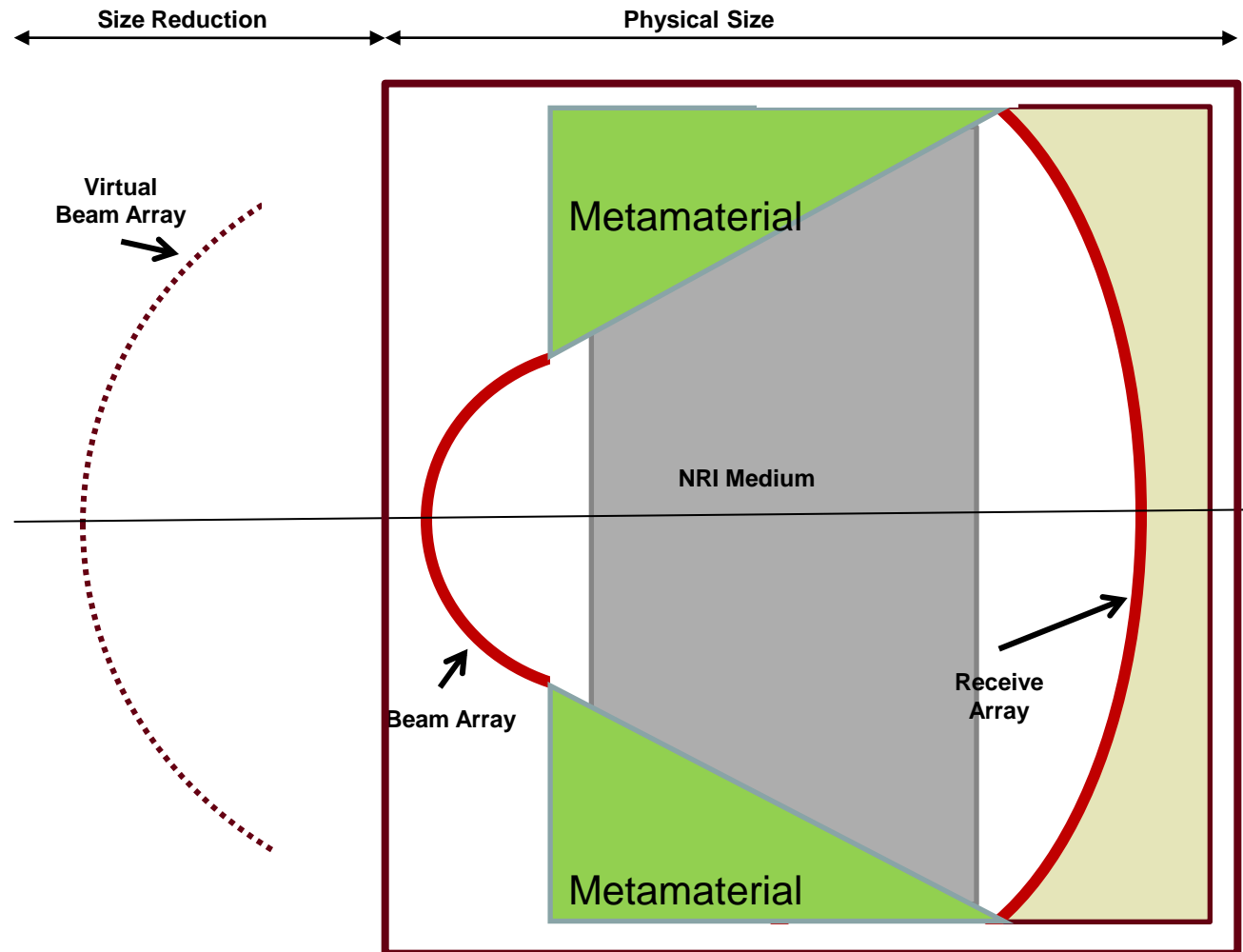
Radiation Pattern of Planar, 2-Fin Structure



Radiation Pattern of 12-Fin Structure



A Metamaterial-Loaded Rotman Lens



- Use negative refractive index medium
- New optics pattern
- Reduced size
- Single ray path



- **Introduction**
- **Metamaterials**
 - Negative Refractive Index
 - Periodic and Random Material
 - Application to Enhanced Dipole Antenna
 - Application to Rotman Lens
- **Metasurfaces**
 - Electromagnetic Band-Gap Surfaces
 - Wideband EBG Surfaces
 - Adaptive and Active Reflection Phase Surfaces
 - Application to Spiral Antennas
 - Application to Cognitive Radar
- **Nanotechnology**
 - Carbon Nano-Tubes
 - CNT Patches
 - Application to Gas Sensors
 - Application to Polarization-Selective Patches
- **Conclusions**



Metasurfaces

Example: Electromagnetic Band Gap (EBG) Surfaces



- EBG structures are usually periodic
- High surface impedance
- Do not support surface waves
- Useful when mounting an antenna close to a ground plane
- EBG structures are compact in size, have low loss, and can be integrated into an antenna

- In phase reflection of the wave
- Band Gap is the frequencies where the reflected phase is between +90 and -90°
- Usually narrowband

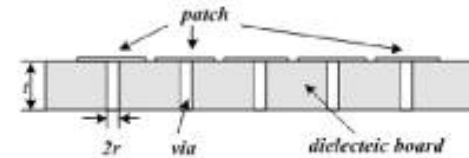
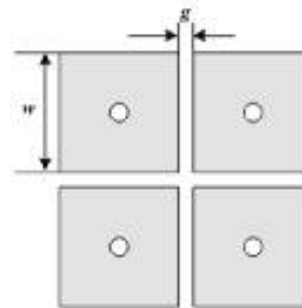
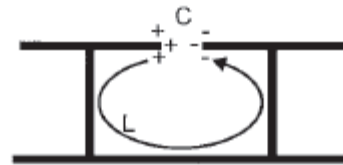
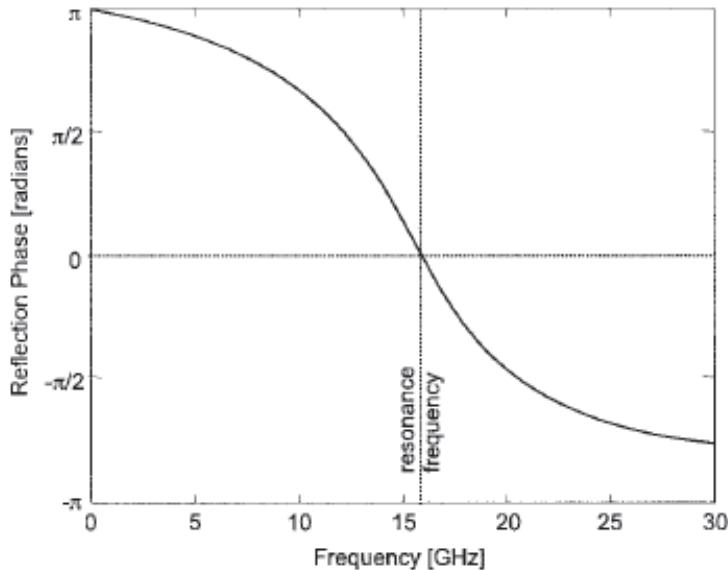
$$Z_s = \frac{j\omega L}{1 - \left(\frac{\omega}{\omega_0}\right)^2}$$

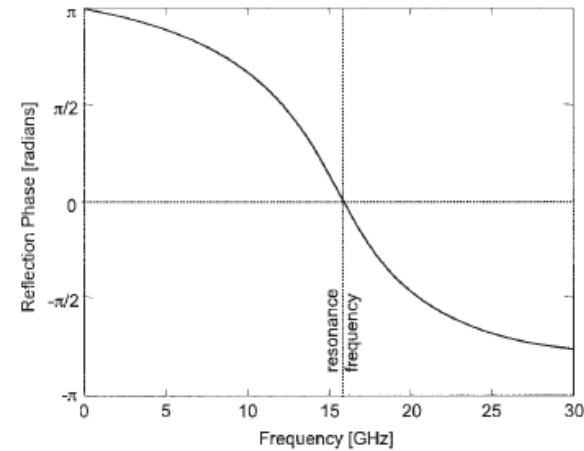
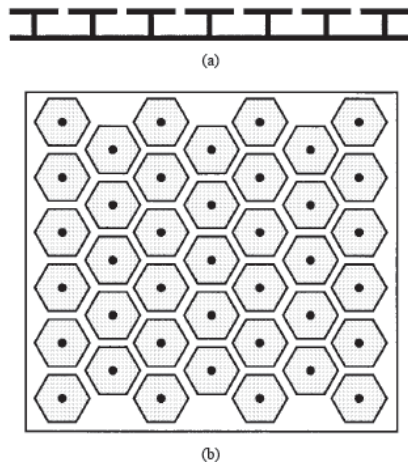
$$\omega_0 = \frac{1}{\sqrt{LC}}$$

$$L = \mu_0 t$$

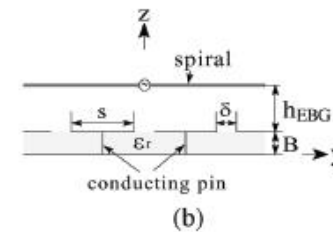
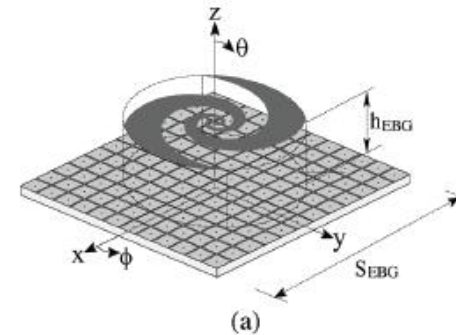
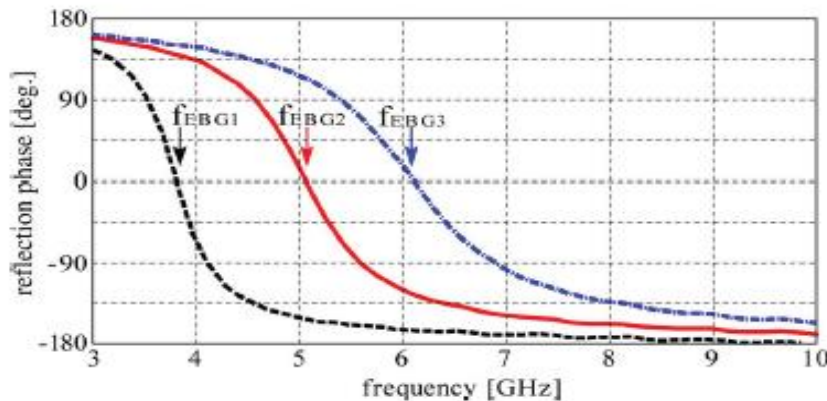
$$C = \frac{W\epsilon_0(1 + \epsilon_r)}{\pi} \cosh^{-1}\left(\frac{2W + g}{g}\right)$$

$$BW = \frac{1}{120\pi} \sqrt{\frac{L}{C}}$$





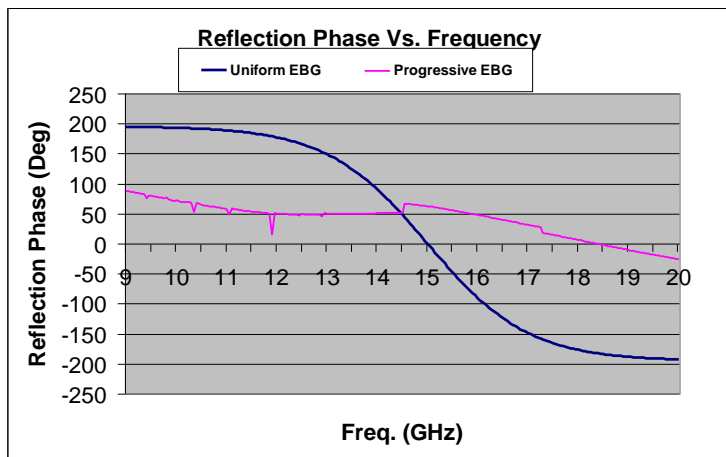
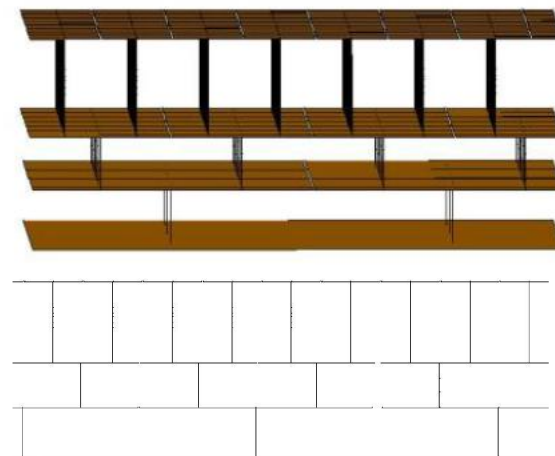
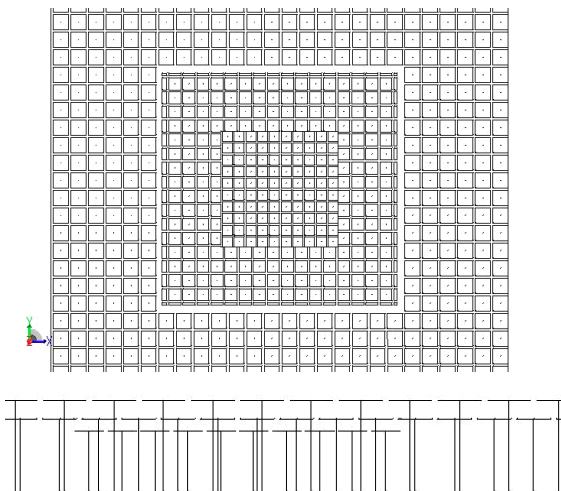
Mushroom EBG Configuration and Reflection Phase*



Variation of Frequency Response of Reflection Phase with Patch Dimensions**

*Sievenpiper et al., IEEE Trans MT&T, Nov 1999

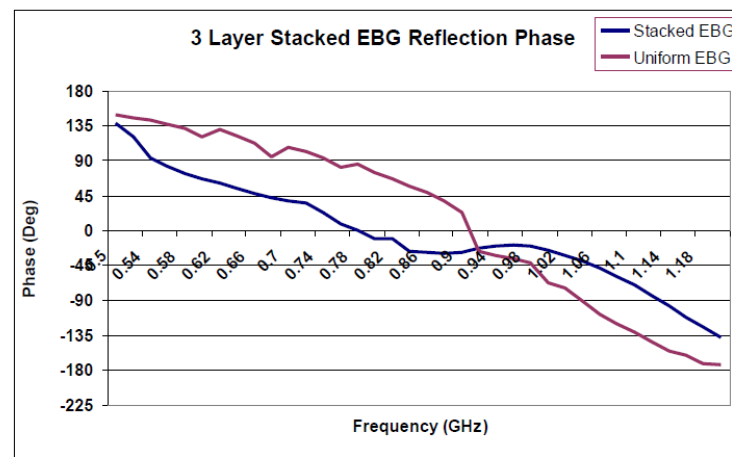
** Nakano et al., IEEE Trans A&P, May 2009



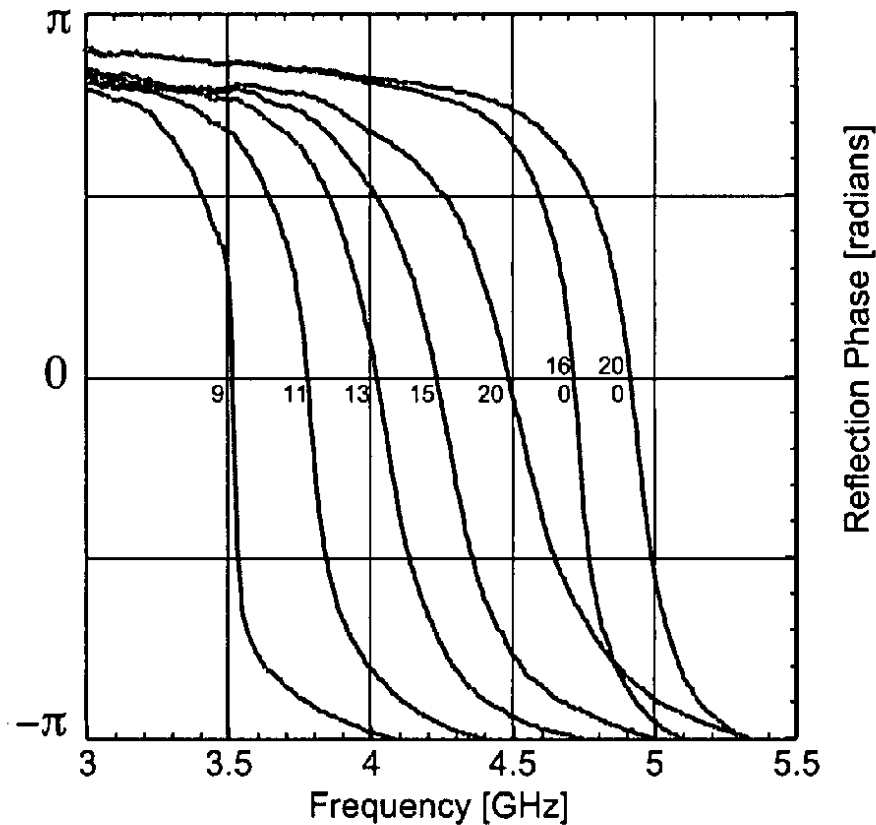
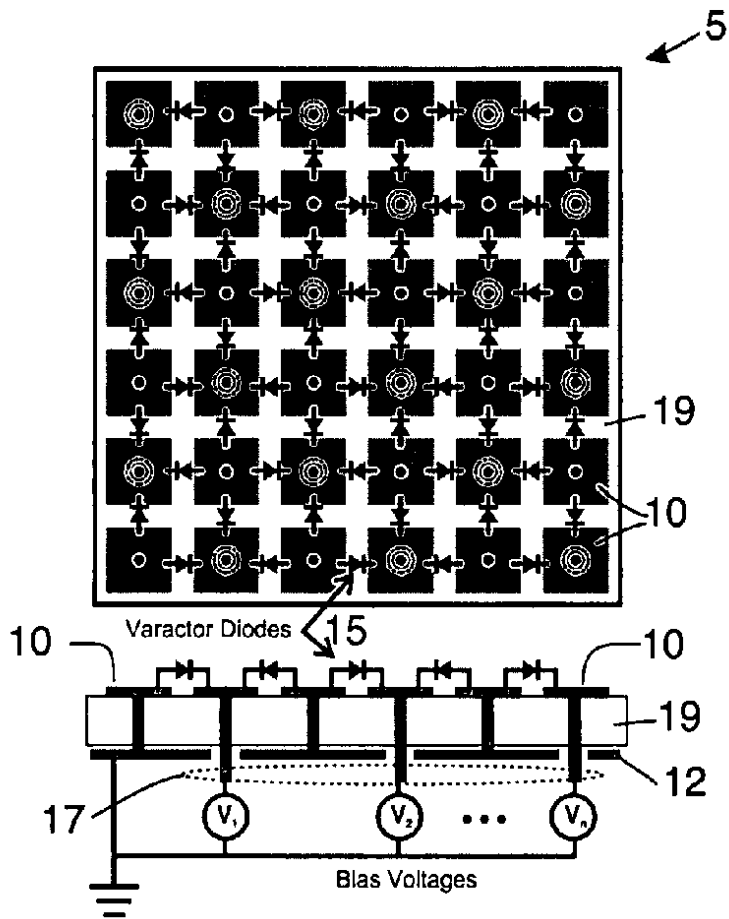
Frequency response of reflection phase for uniform (fast) and progressive (slow) EBG*

*Zaghloul, Palreddy, Weiss, EuCAP 2011

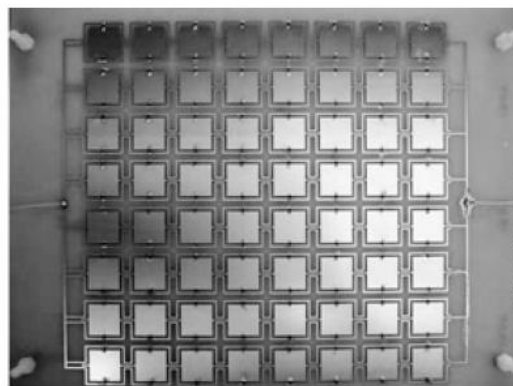
** Palreddy, Zaghloul, Lee, EuCAP 2012



Frequency response of reflection phase for uniform (fast) and stacked (slow) EBG**

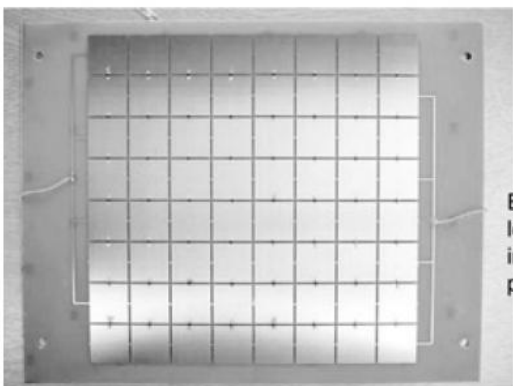


Tunable EBG surface using varactor diodes



EBG1
length of square element: 20 mm
gap patch and loop: 1.7 mm
thickness of square loop: 1 mm
periodicity: 29.5

a

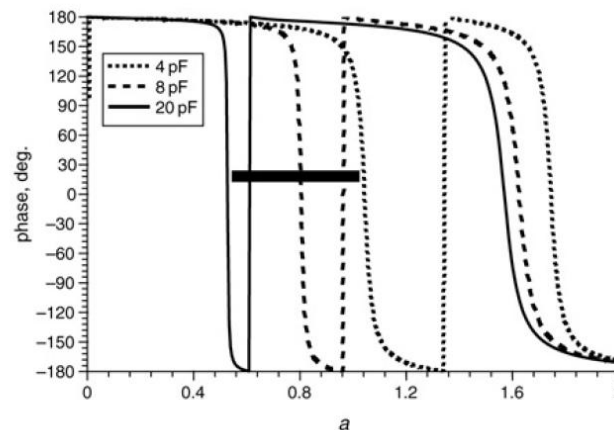


EBG2
length of square element: 28 mm
inter-element spacing: 1.5 mm
periodicity: 29.5 mm

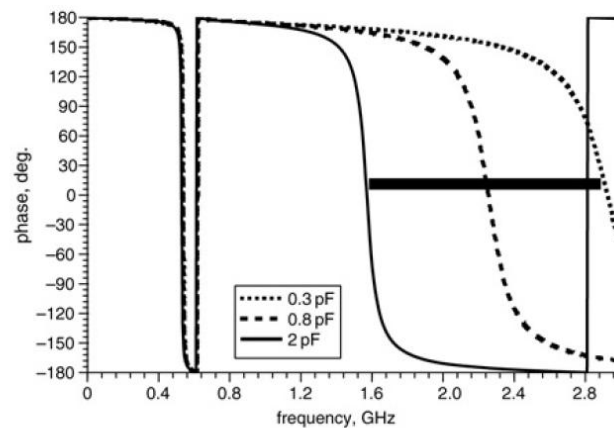
b

Fig. 1 Illustration of unit cell of active EBG

a EBG1
b EBG2



a

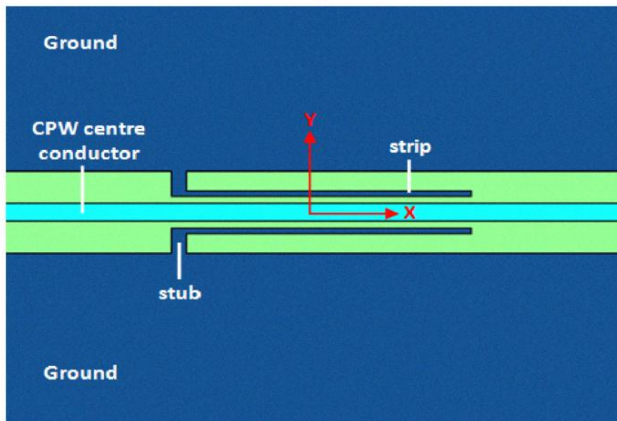


b

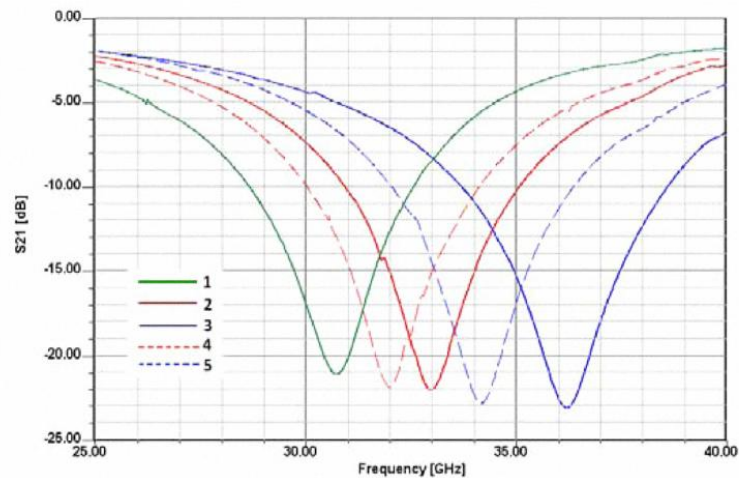
Fig. 2 Simulated reflection phase for tunable EBG

a EBG2 tuned from 4 to 20 pF
b EBG1 tuned from 0.3 to 2 pF

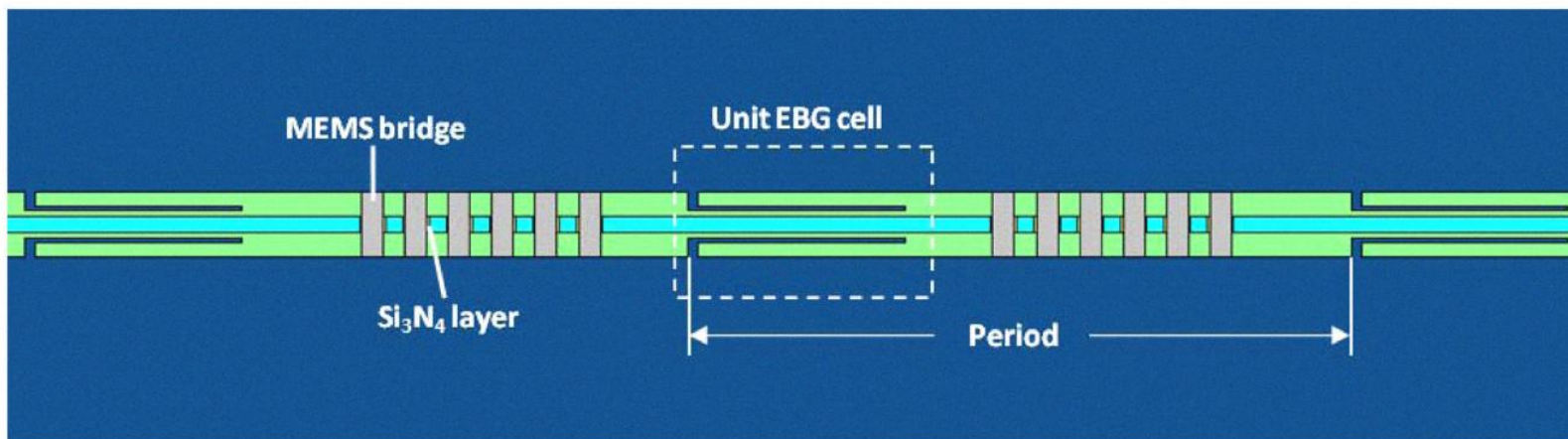
EBG surface independently tuned over two separate frequency bands using dual layer with varactor diodes



Schematic of unit EBG cell

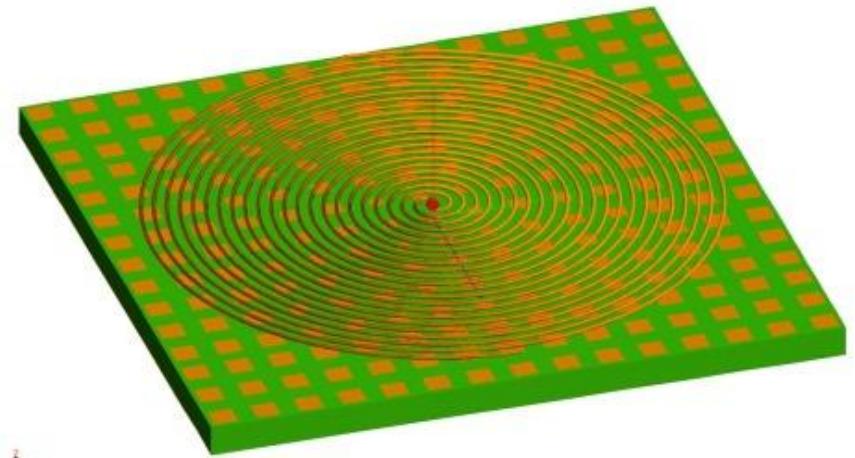
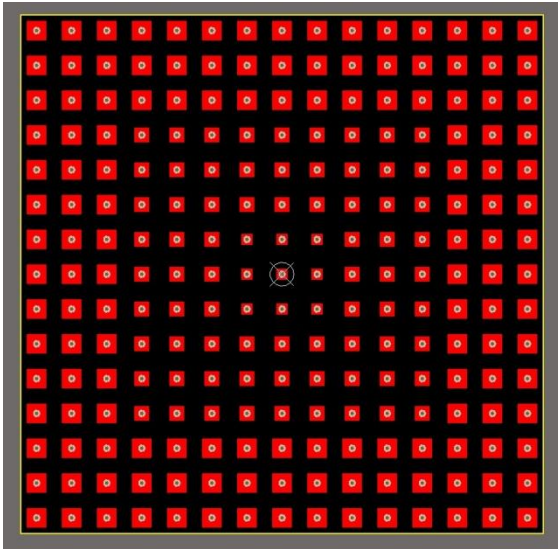


S21-Parameter for unit EBG cell



Top view of tunable structure

- Formed by cascading Uniform EBGs of same height
- Resonate close to one another
- Has a wider band gap than regular EBG

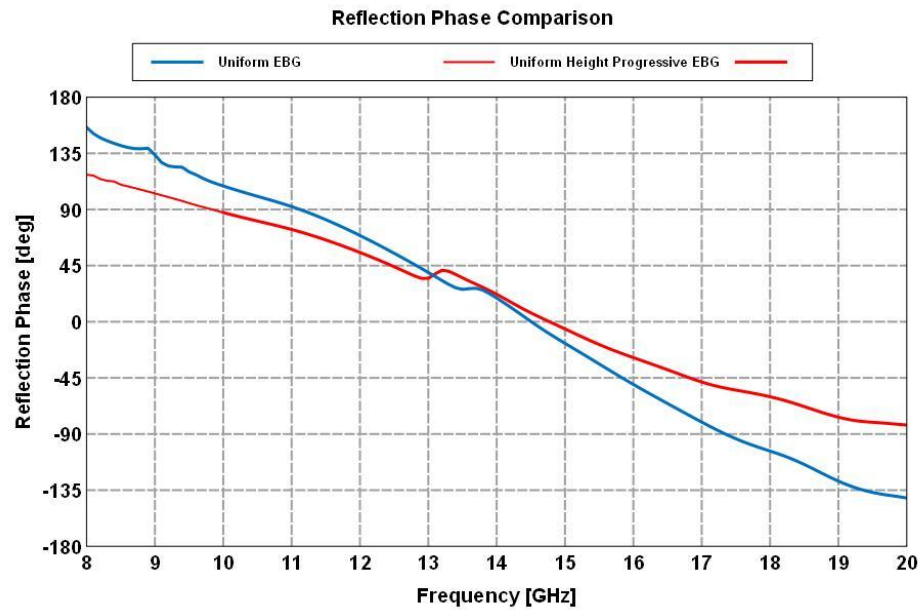




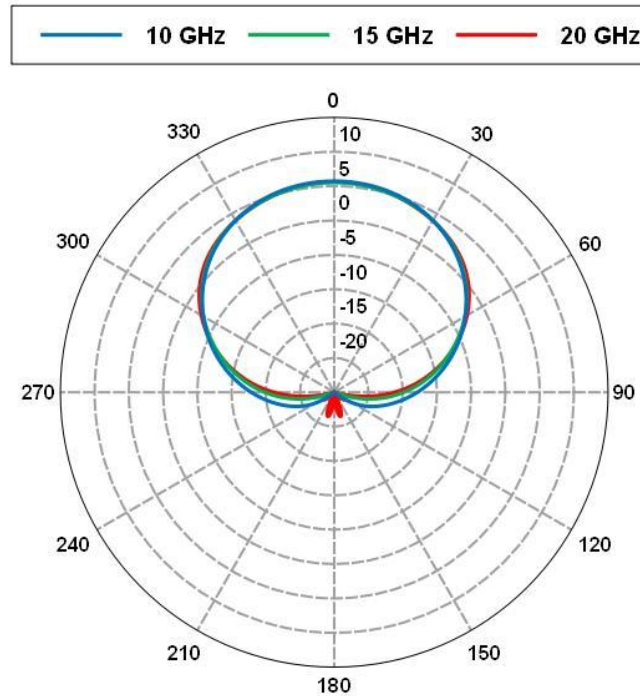
Reflection Phase Comparison



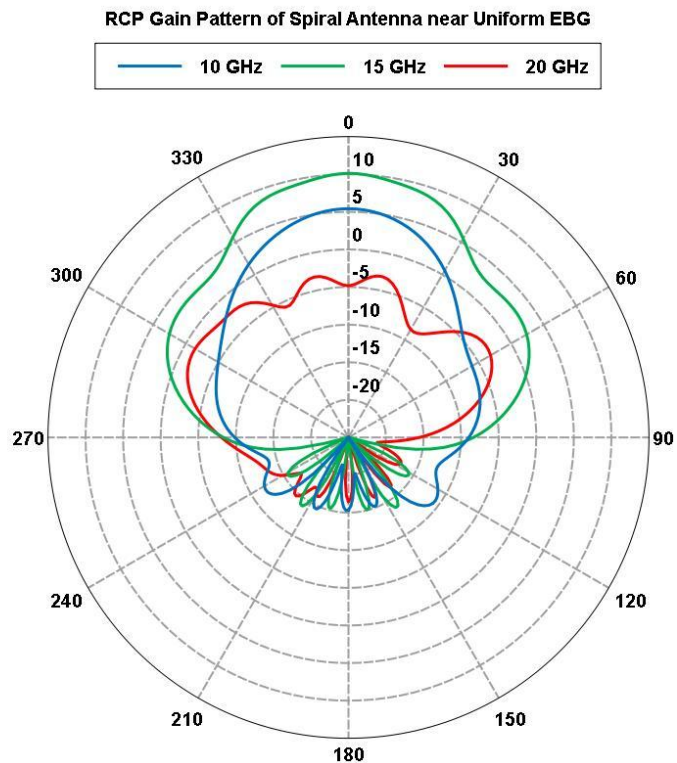
- Computed using FEKO
- Reflection phase computed just above the EBG surface
- Notice that the Progressive EBG structure has wider band gap.



RCP Gain Pattern of Spiral Antenna in Free Space



Gain patterns of the spiral antenna in free space



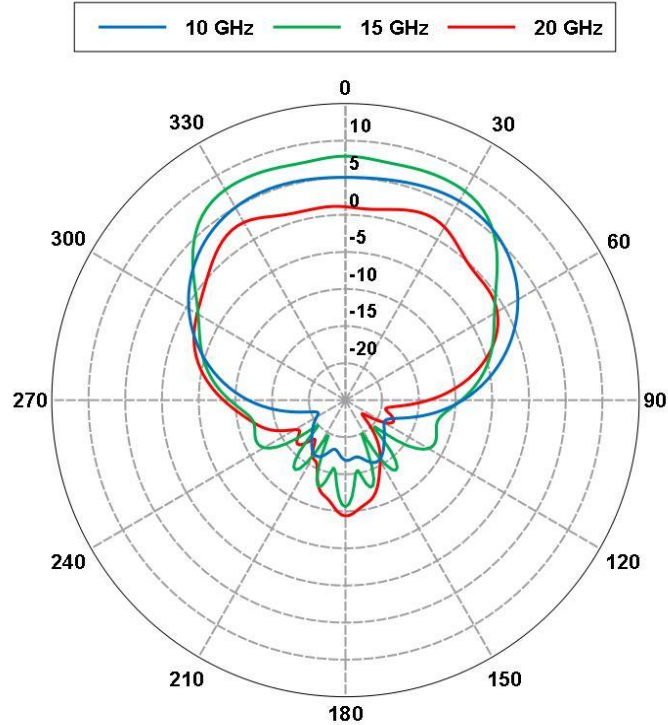
Gain patterns of the spiral antenna near uniform EBG



Spiral Antenna near Progressive EBG



RCP Gain Pattern of Spiral Antenna near Progressive EBG

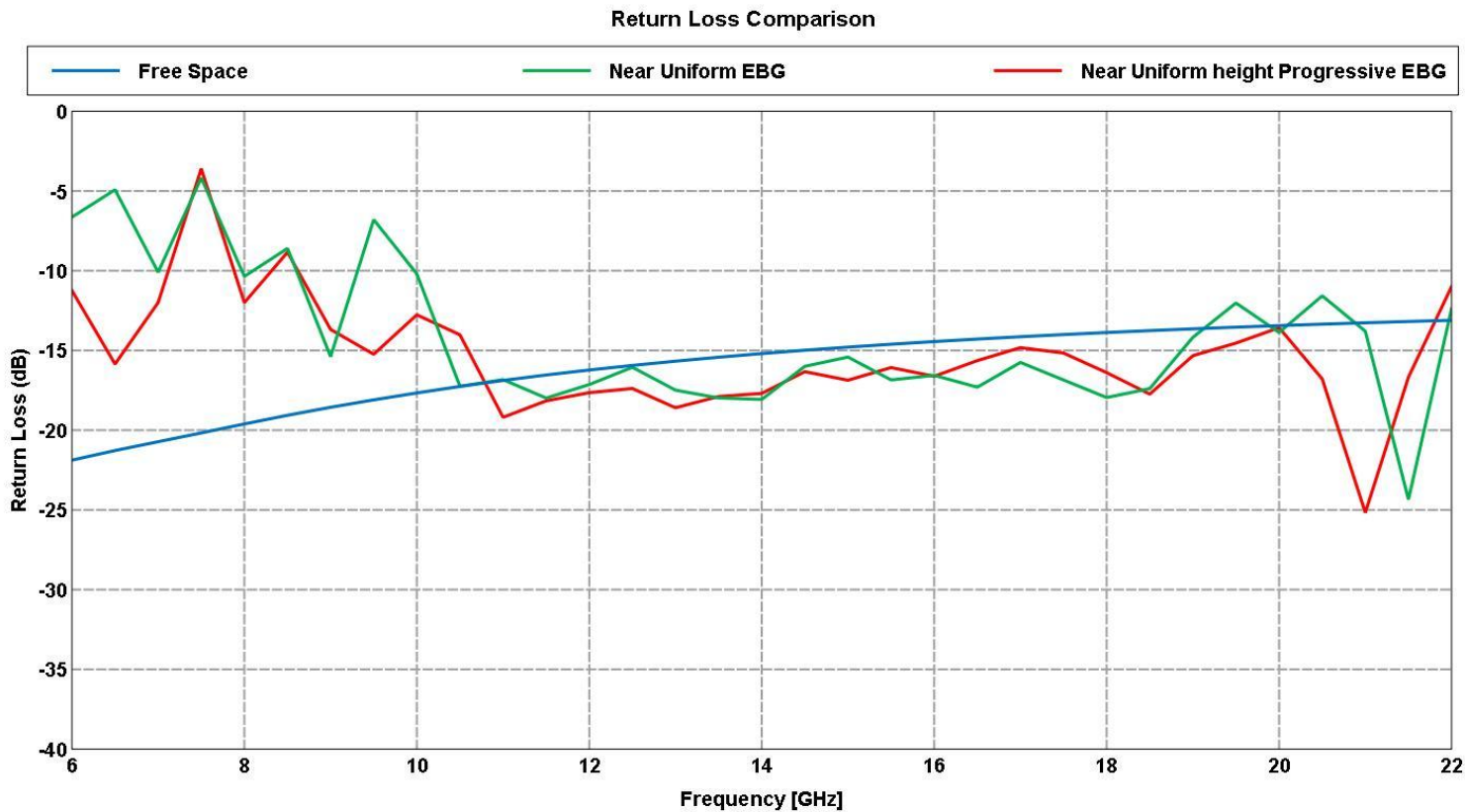


Total Gain [Phi = 0 deg] - Progressive EBG Structure on Duroid for Fab 9-2-12 with Spiral Antenna

Gain patterns of the spiral antenna near progressive EBG



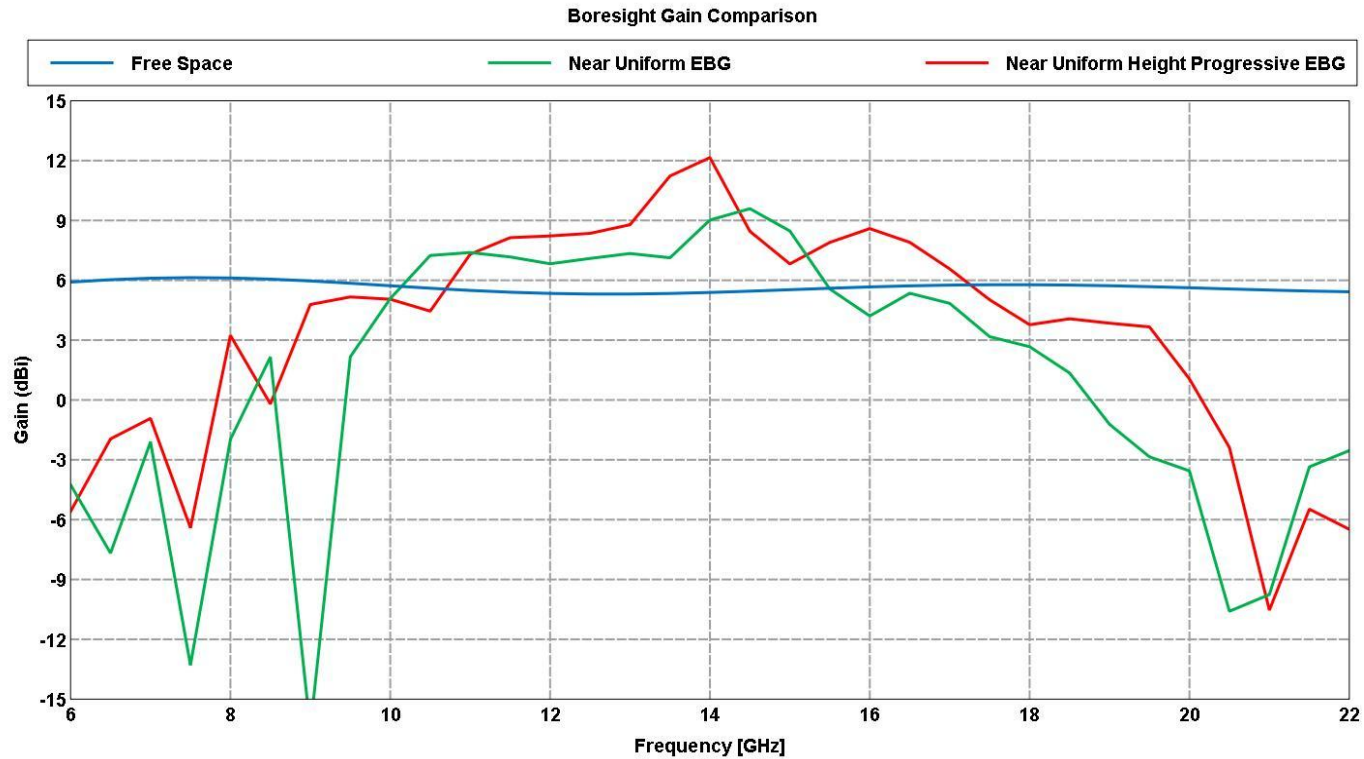
Return Loss Comparison



Return Loss comparison of the spiral antenna under different loading conditions



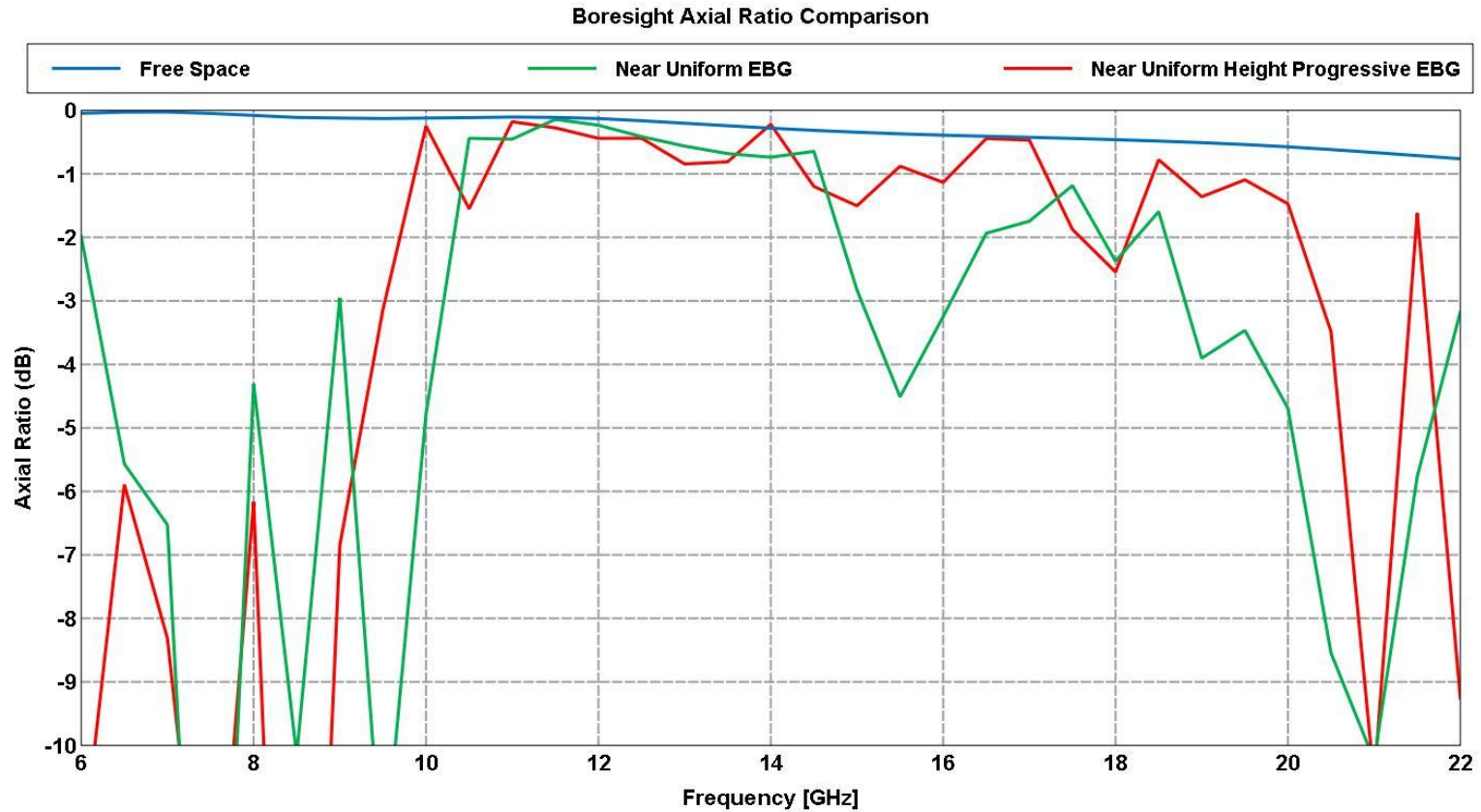
Boresight Gain Comparison



Boresight gain comparison of the spiral antenna under different loading conditions



Axial Ratio Comparison



Boresight axial ratio comparison of the spiral antenna under different loading conditions



Features of Spiral Antenna near Progressive EBG



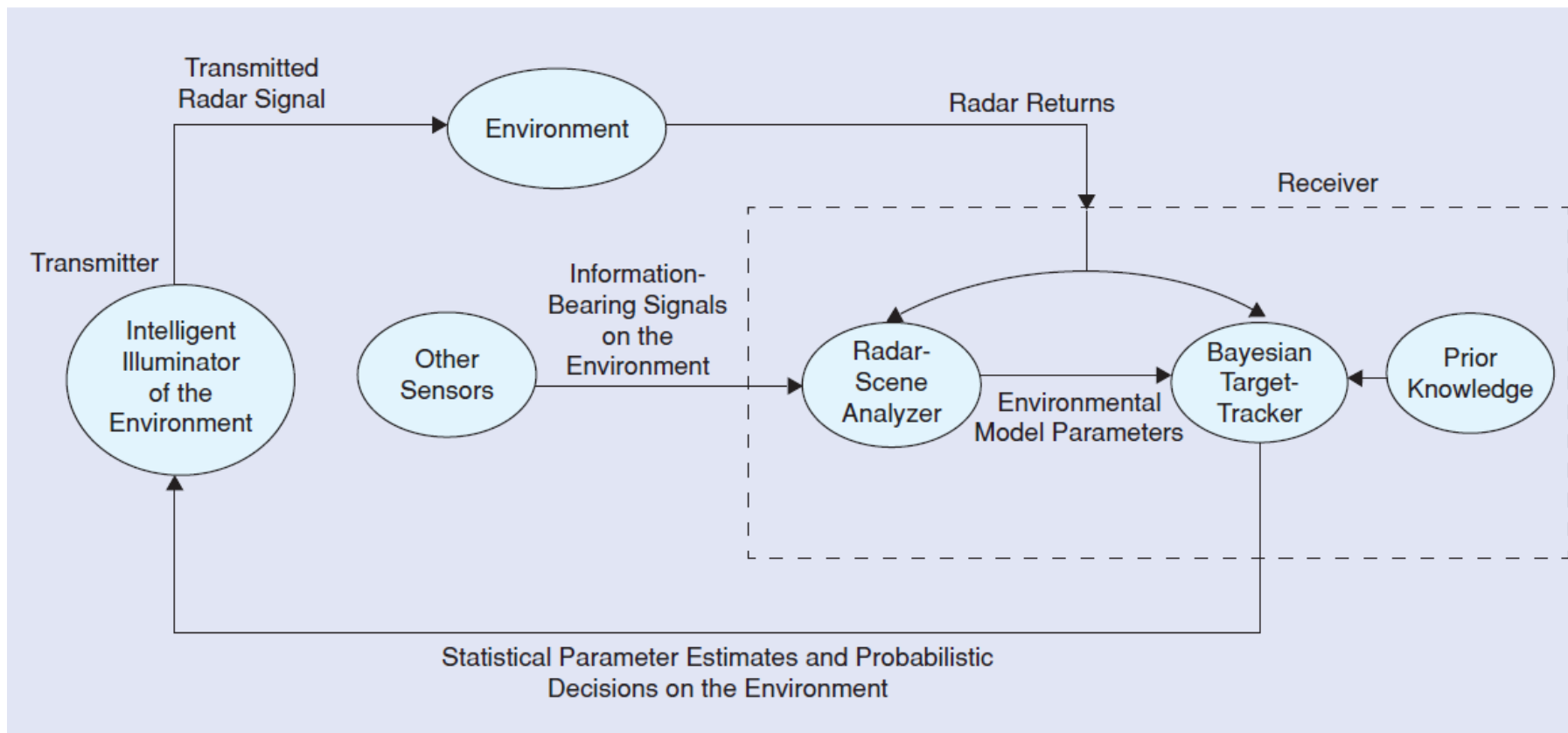
- Higher gain and higher front-to-back ratio with progressive EBG
- Better boresight axial ratio performance with progressive EBG than Uniform EBG
- Uniform height progressive EBG structure has a wider band gap, compared to the regular EBG structure
- Accomplished with low profile that is afforded by the reflection phase characteristics of the broadband EBG
- This low profile is in contrast with the higher profile design that uses PEC-backed or absorber-backed cavities
- Gain patterns of the antenna near progressive EBG are cleaner & smoother, like the case in free space, compared to the case near uniform EBG



Application of Adaptive Metasurfaces to Cognitive Radar



- Cognitive Radar is based on learning through interactions of the radar with the environment
- Information is facilitated by feedback from the receiver to the transmitter
- Information on target is deduced through processing of radar returns
- Environment or channel data include reflection phase and resonance frequencies of surfaces, which constitute part of the feedback from the receiver to the transmitter
- Adaptive reflection phase control can be a key function



Block diagram of cognitive radar viewed as a dynamic closed-loop feedback system*

* S. Haykin, "Cognitive Radar, A way of the future," *IEEE Signal Processing Magazine*, January 2006



Quotes from S. Haykin



- For the radar to be cognitive, adaptivity has to be extended to the transmitter too
- The function of the radar-scan analyzer is to provide the receiver with information on the environment
- The selection of waveforms to be used for adaptive radar transmission is application dependent
- There is much that we can learn from the echo-location system of a bat
- An echo-locating bat can pursue and capture its target with a facility and success rate that would be the envy of a radar engineer



Adaptive Reflection Phase

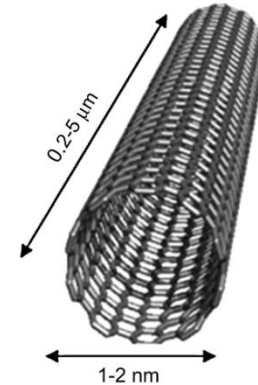


- Adaptively control the environment, primarily reflection function
- Function of phase variation can be controlled by transmitter and shared by receiver
- Narrow-band fast phase change or wide-band slow phase change versus frequency
- Introduces false target information in radar jamming systems
- Can be effective in Digital Radio Frequency Memory (DRFM) techniques

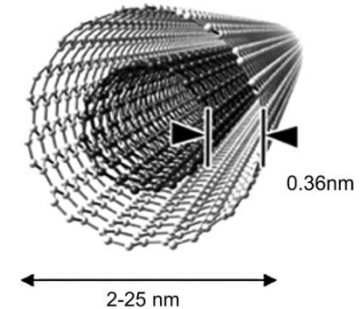
- **Introduction**
- **Metamaterials**
 - Negative Refractive Index
 - Periodic and Random Material
 - Application to Enhanced Dipole Antenna
 - Application to Rotman Lens
- **Metasurfaces**
 - Electromagnetic Band-Gap Surfaces
 - Wideband EBG Surfaces
 - Adaptive and Active Reflection Phase Surfaces
 - Application to Spiral Antennas
 - Application to Cognitive Radar
- **Nanotechnology**
 - Carbon Nano-Tubes
 - CNT Patches
 - Application to Gas Sensors
 - Application to Polarization-Selective Patches
- **Conclusions**

- Carbon nanotubes (CNTs) are sheets of graphene rolled up as hollow cylinders
 - Typical diameter range of 1 –2 nm for single wall CNTs (SWCNT) and 2 –25 nm with 0.4 nm spacing (van der Waals gap) between concentric shells for multi wall CNTs (MWCNT)
 - Lengths > 1 cm have been achieved for single tubes
 - Threads of long CNTs can be woven together to increase length and overall diameter
- Chirality (orientation of rolled-up graphene sheets) determines metallic or semiconducting nature of SWCNTs
 - Zigzag – semiconducting, Armchair – metallic, Chiral – mostly semiconducting
 - MWCNTs are always metallic / MWCNT bundles exhibit multiple conducting channels in parallel and are better electrical conductors than SWCNT bundles
- CNTs have long mean free electron paths (on order of several μm vs. nm for Cu at room temperature)
 - Leads to **low resistivity** and **possible ballistic transport** over short lengths
- Electrons conduct through the π -bond of carbon atoms
 - Skin effect can be ignored up through the THz frequency range

Single Wall



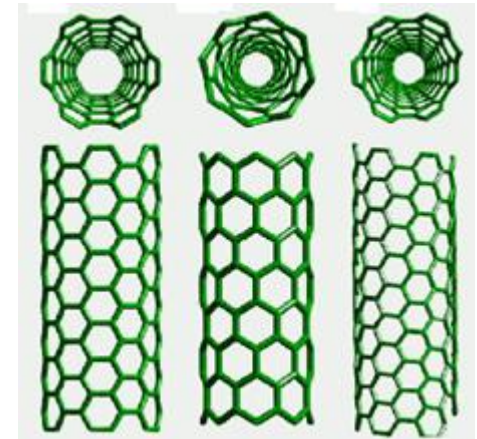
Multi Wall



Armchair

Zigzag

Chiral



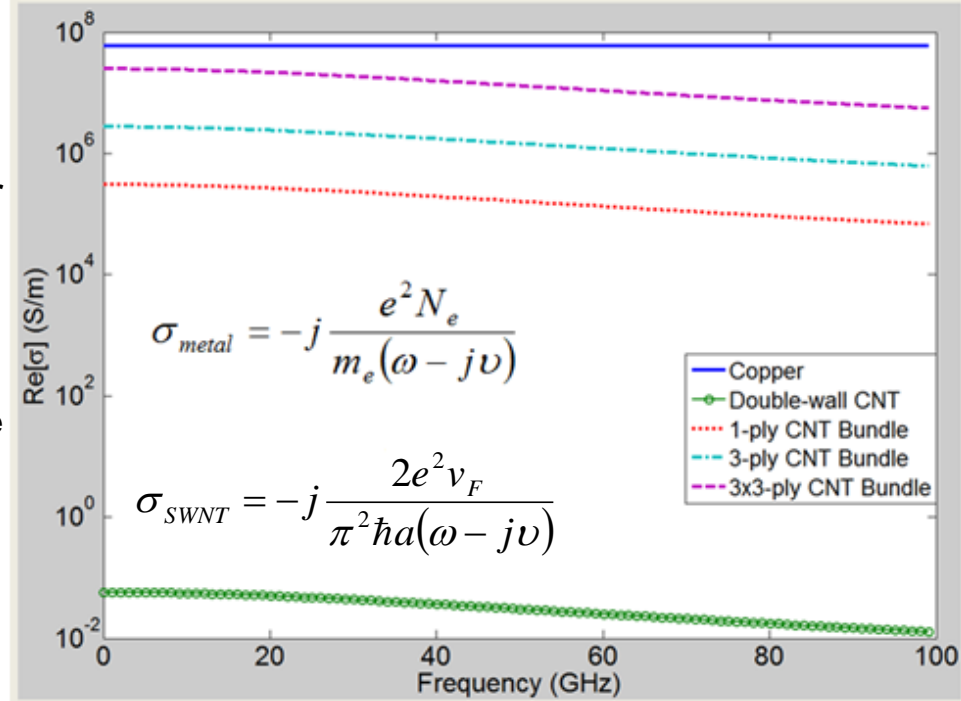


Carbon Nanotube Thread Conductivity Simulation



- Conductivity simulated for thin copper cylinder, double-wall carbon nanotube and 1-ply, 3-ply and 3x3 (9)-ply carbon nanotube thread
 - 3.4 Å van der Waals spacing between nanotubes in CNT thread
- CNT thread predicted to yield orders of magnitude higher conductivity above single carbon nanotube
- Simulations agree well with measured resistivity of CNT thread (1e-4 Ω-cm → σ ≈ 1e6 S/m), and confirm known conductivity of copper (~5.96e7 S/m)
- Increasing CNT thread/rope ply (diameter and conductive paths) should yield improved conductivity

Conductivity vs. Frequency



Number of Carbon Nanotubes in Rectangular CNT Bundle

$$N_w = \frac{2(R-a)}{x}; N_L = \frac{2(R-a)}{(\sqrt{3}/2)x} + 1$$

$$N_{total} = N_w \cdot N_L - \frac{N_L}{2}; N_{outer} = 2 \cdot (N_w + N_L)$$

Approximate Number of Carbon Nanotubes in Circular CNT Bundle / Thread

$$\frac{A_{circle}}{A_{square}} = \frac{\pi R^2}{2R \cdot 2R} = \frac{\pi}{4}; N_{total} \approx \frac{\pi}{4} N_{total}$$

Conductivity of Double-wall Nanotube

$$\sigma_{MWNT} = \sum_{q=1}^N \sigma_{SWNT}^{(q)}$$

$$\sigma_{DWNT} \approx 2\sigma_{SWNT}$$

Conductivity of CNT Bundle / Thread

$$\sigma_{Bundle} \approx N_{total} \cdot \sigma_{DWNT}$$

$e = 1.602e-19$ coulombs $m_e = 9.11e-31$ kg
 $N_e = 8.46e28$ electrons/m $v = (2.47e-14)$
 $\hbar = 1.0546e-34$ m kg/s $v_F = 9.71e5$ m/s
 $R =$ CNT thread radius $a =$ CNT radius
 $x =$ intertube CNT spacing = $2a + 3.4 \text{ \AA}$

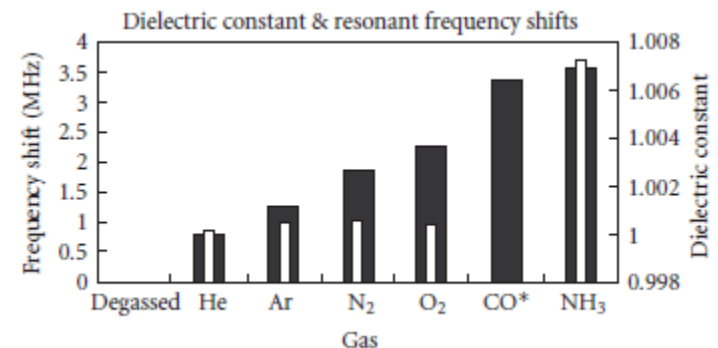
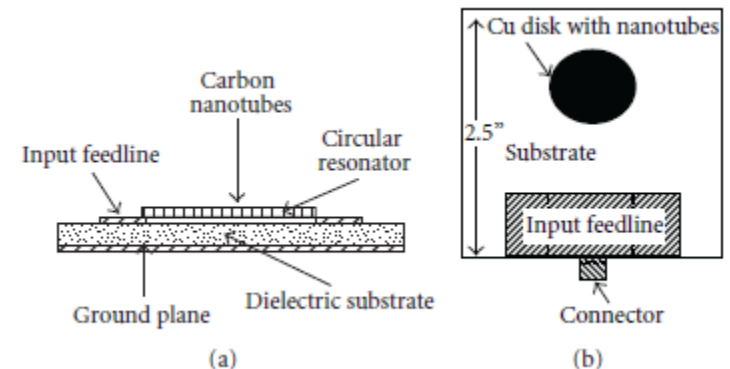
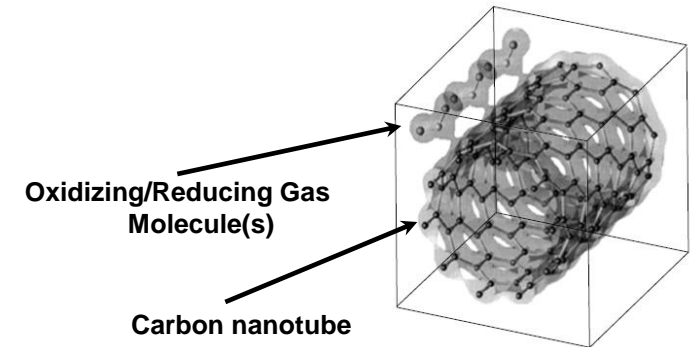
Prototype	Radius (μm)
Double-wall CNT	0.005
1-ply CNT thread	12.5
3-ply CNT thread	37.5
3x3-ply CNT thread	112.5
30-gauge Cu wire	127.5
15-gauge Cu wire	725



Carbon Nanotube Gas Sensor Background



- When subjected to certain oxidizing/reducing gases, ϵ_r and σ of CNTs are altered
 - Examples: He, Ar, N₂, O₂, NH₃
- Charge transfer between the reacting gas molecules and the CNTs are the most likely mechanism for this occurrence
 - Gas molecules act as either electron donors or acceptors to CNTs
- Process is reversible (ϵ_r and σ return to original values over recovery time)
- CNT gas sensor achieved by coating a microwave cavity resonator with a thin layer of randomly scattered SWNTs and/or aligned MWNTs
 - Resonator frequency shifts by small, but measurable amount in direct response to the change in ϵ_r and σ caused by the presence of the reacting gas



Goal: Incorporate CNT gas sensing capabilities with RF properties to yield complete lightweight, durable wireless gas sensor

- Radiating slots produce broadside radiation pattern
 - When substrate thickness, t , is small, radiation is approximated by horizontal magnetic currents circulating the perimeter of the patch over a ground plane
- 50 Ω microstrip line (impedance matched to antenna feedpoint) provides RF energy to patch through aperture in ground plane

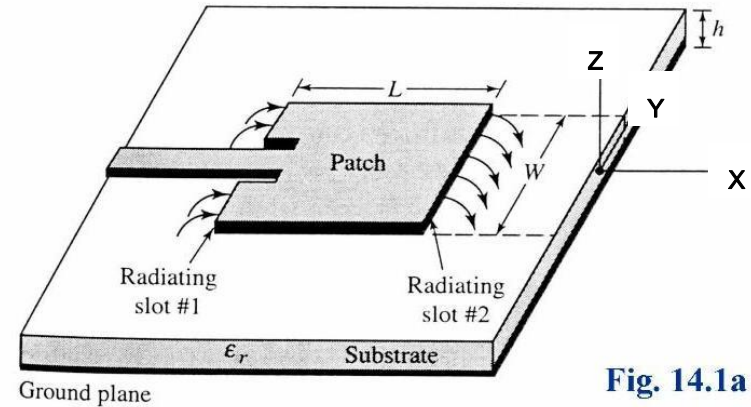


Fig. 14.1a

Copyright © 2005 by Constantine A. Balanis
All rights reserved

Chapter 14
Microstrip Antennas

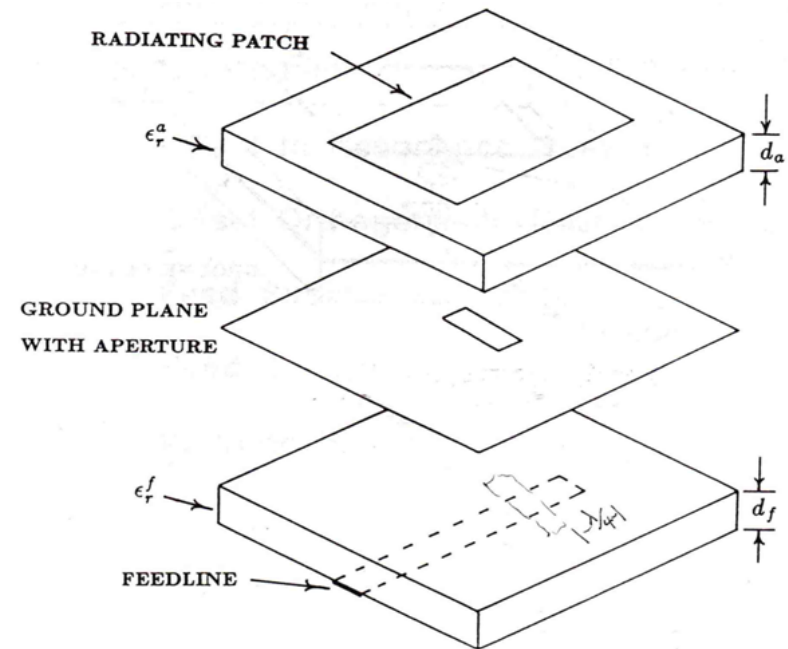
$$1) \quad W = \frac{1}{2f_r \sqrt{\mu_0 \epsilon_0}} \sqrt{\frac{2}{\epsilon_r + 1}} = \frac{c}{2f_r} \sqrt{\frac{2}{\epsilon_r + 1}}$$

$$2) \quad \epsilon_{eff} = \frac{\epsilon_r + 1}{2} + \frac{\epsilon_r - 1}{2} \left[1 + 12 \frac{t}{W} \right]^{-1/2}$$

$$3) \quad \frac{\Delta L}{t} = 0.412 \frac{(\epsilon_{eff} + 0.3) \left(\frac{W}{t} + 0.264 \right)}{(\epsilon_{eff} - 0.258) \left(\frac{W}{t} + 0.8 \right)}$$

$$4) \quad \lambda^{cm} \approx \frac{30}{f_r \text{ (in GHz)}}$$

$$L = \frac{\lambda}{2\sqrt{\epsilon_{eff}}} - 2\Delta L$$

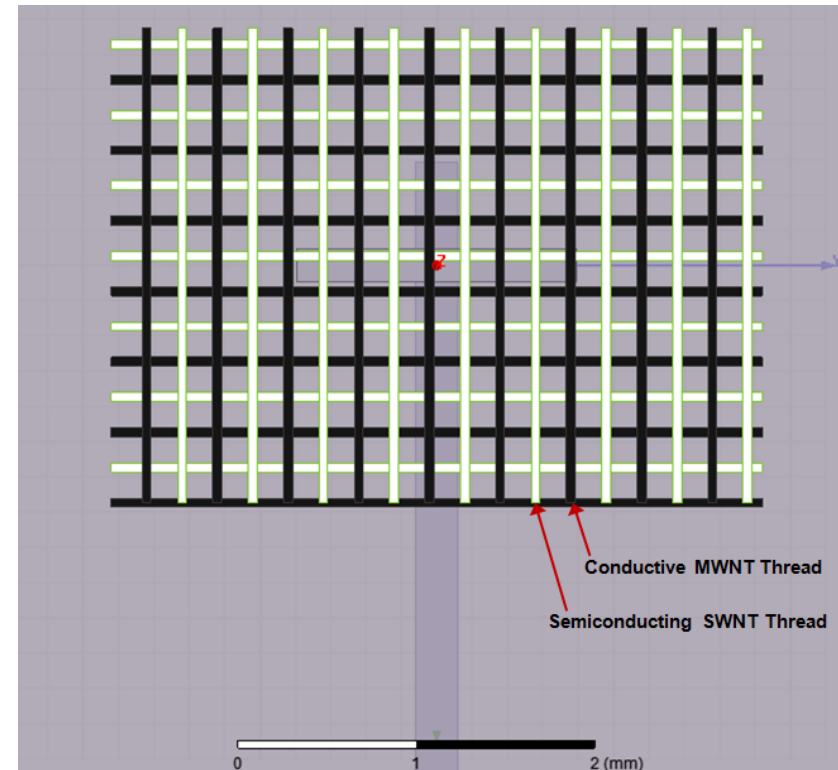




Carbon Nanotube Meshed Thread Patch Antenna Concept



- Apply carbon nanotube thread/yarn to create meshed patch antenna structure
- Alternate thread in mesh with highly conductive MWNT thread (RF radiators) and semiconducting SWNT thread (dielectric buffer / “gas sensing” mechanism)
 - MWNT threads are main conductive elements for radiating meshed thread patch antenna
 - SWNT threads have high # of defects to limit their conductivity and serve as dielectric buffer threads
 - Defect sites on SWNT threads provide more locations for reactive gas molecules to donate or accept electrons → increases gas sensing mechanism
- In the presence of oxidizing/reducing gases, ϵ_r of SWNT dielectric buffer threads will change and resonant frequency of patch antenna will shift

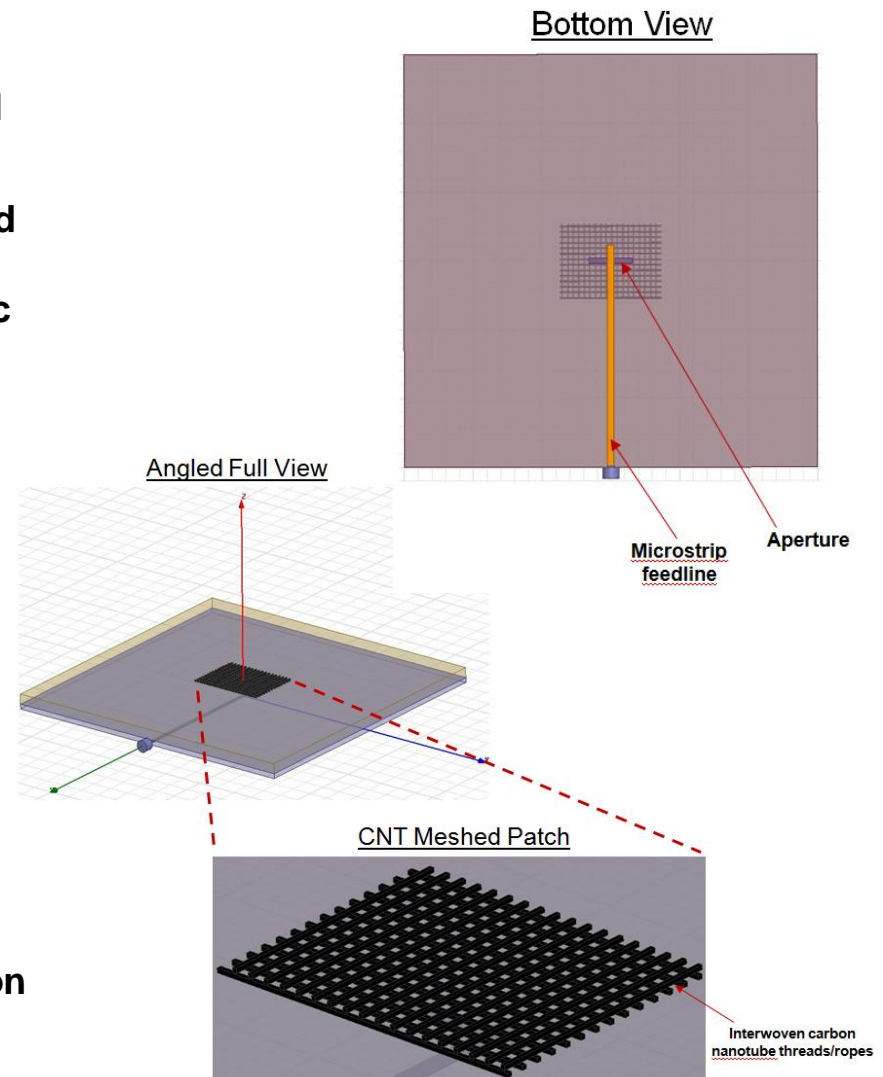


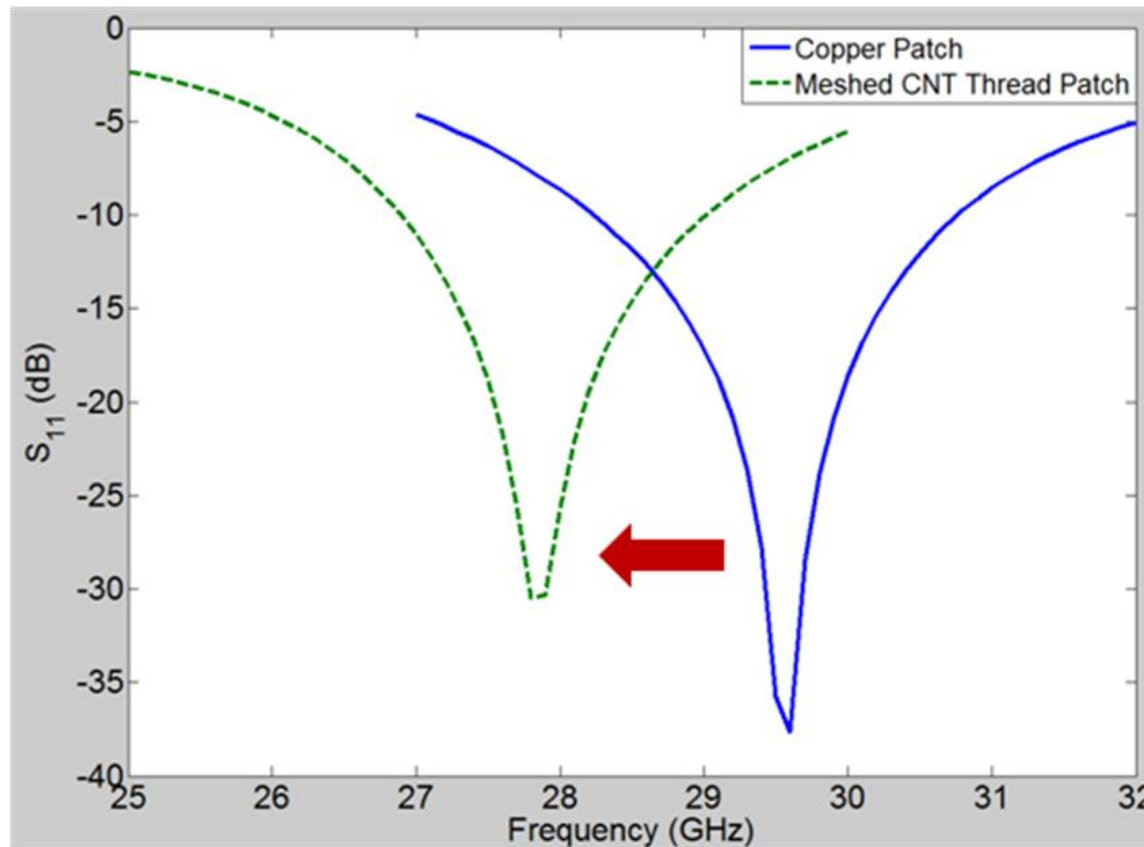


Meshed Carbon Nanotube Thread Patch Antenna Design

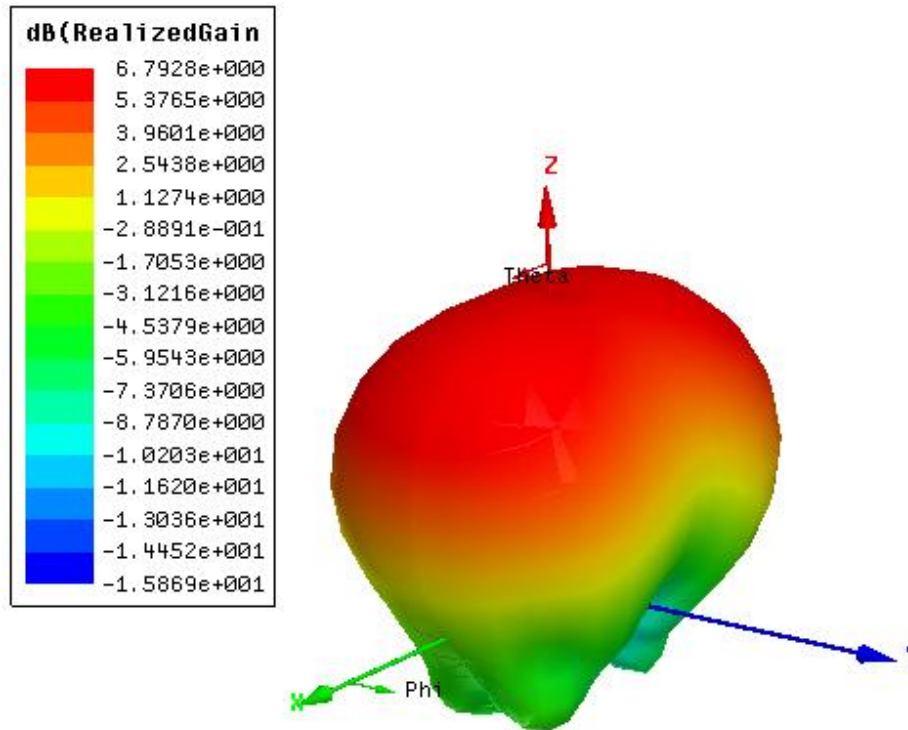


- Ka-band antenna design ($f_0 \approx 30$ GHz)
- 2.7 x 3.7 mm aperture-coupled meshed CNT thread patch antenna
- Patch constructed from 50 μm diameter CNT thread (alternating between high-conductivity MWNT threads and low-conductivity, high-defect dielectric buffer SWNT threads) spaced $\sim \lambda/67$ apart
- Conductive MWNT threads assigned approximate conductivity of $\sigma = 1\text{e}6$ S/m; defects in CNT walls (resistive barriers) and quantum level effects (CQ, LK) not accounted for in this simulation
- Semiconducting / dielectric buffer SWNT threads assigned dielectric constant, $\epsilon_r = 5$, based on measured data from literature
- RT/Duroid 6010 ($\epsilon_r = 10.2$, $t = 10$ mil) for feedline substrate, RT/Duroid 5870 ($\epsilon_r = 2.33$, $t = 20$ mil) for patch substrate
- Feedline ($l = 1590$ μm , $w = 190$ μm) and ground plane constructed from copper to reduce simulation complexity \rightarrow future cases will explore effect of using CNT meshed thread



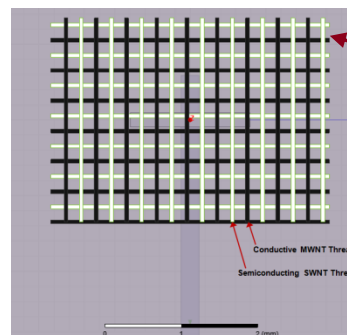


- **Meshed CNT thread patch** design yields center frequency shift (f_0) and bandwidth reduction when compared with **traditional solid copper patch** design
 - 2 GHz (7%) f_0 shift: from **29.6 GHz** to **27.85 GHz**
 - 400 MHz (~16 %) bandwidth ($S_{11} = -10$ dB) reduction: from **2.5 GHz** to **2.1 GHz**

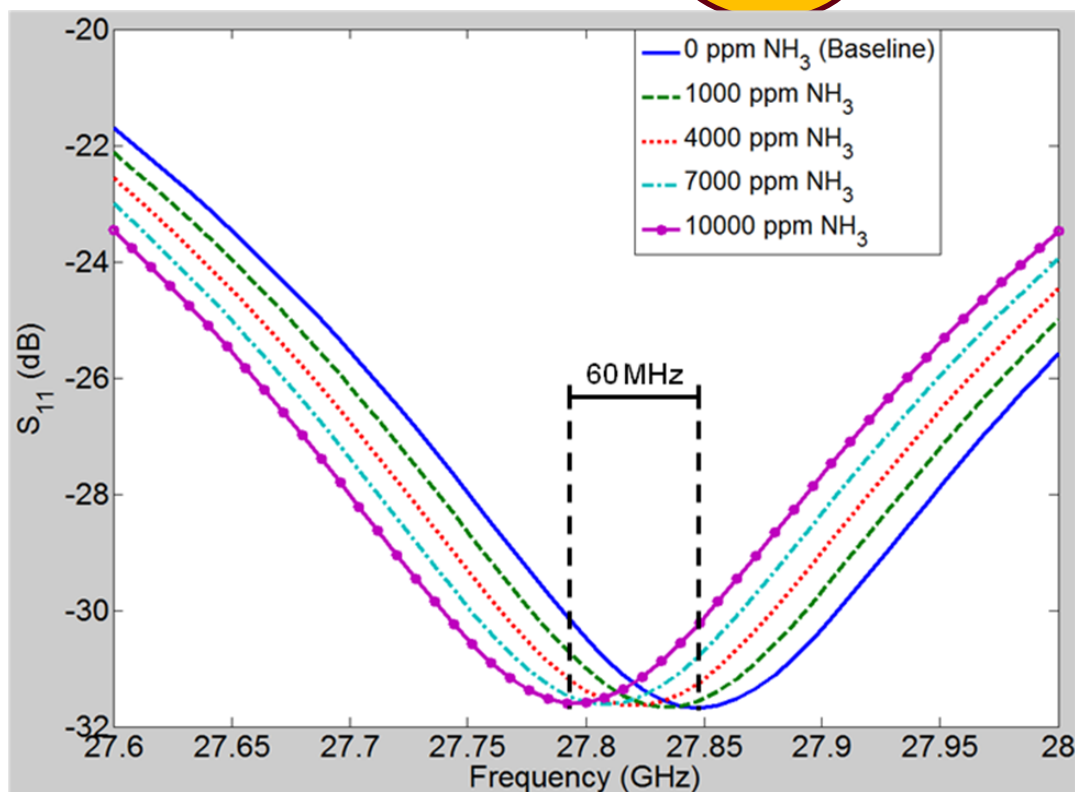


- Broadside radiation pattern maintained with CNT meshed patch antenna
- **Meshed CNT thread patch** design yields small gain reduction when compared with **traditional solid metal patch** design
 - 0.46 dB (~7 %) reduction: from **6.79 dBi** to **6.33 dBi**
 - Gain reduction likely from resonance shift observed in S11 simulation

- From experimental observation, permittivity (ϵ_r) of a thin layer of semiconducting SWNTs increases linearly when in the presence of increasing concentrations of ammonia gas (NH_3)
- Estimated change from $\epsilon_r = 5$ to $\epsilon_r = 5.15$ in presence of 1000 ppm of NH_3 , then $\epsilon_r = \epsilon_r + 0.15$ with each additional 3000 ppm NH_3
 - Permittivity changes applied to SWNT thread model to simulate gas sensing for meshed thread patch antenna
- Small, but measurable resonant frequency shift predicted to occur with increasing concentrations of NH_3 around the meshed CNT thread patch antenna
 - -60 MHz shift in f_0 , from 27.84 GHz to 27.78 GHz
- Frequency shift is small enough to guarantee continuous bandwidth for TX/RX communications functionality
- Adding PABS to SWNT will increase the sensitivity of gas detection with ability to sense very low, and more practical levels

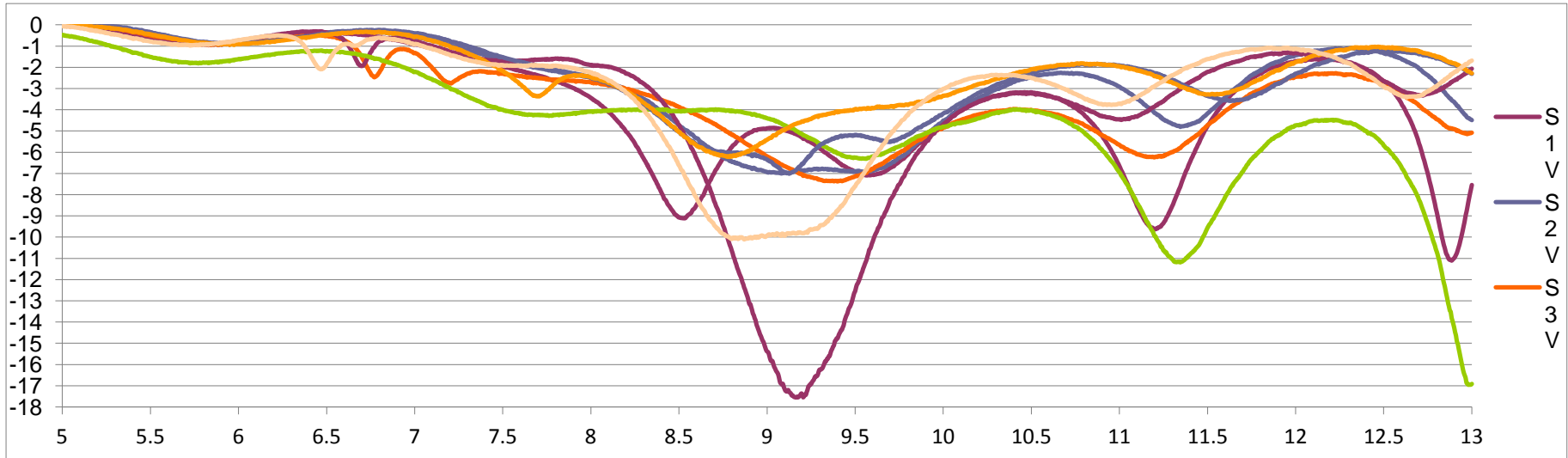


ϵ_r of semiconducting SWNT buffer threads varied from 5 to 6 in 0.15 increments to simulate increasing concentrations of NH_3 gas

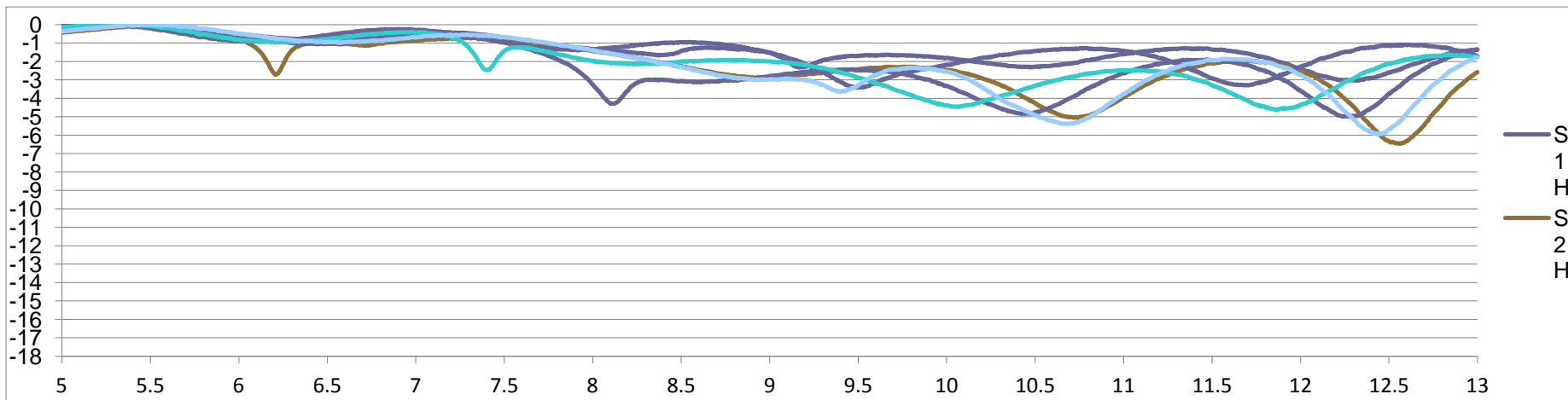




Polarization Selectivity In CNT Patch Antennas



Return Loss for Co-Aligned CNT Patch



Return Loss for Cross-Aligned CNT Patch



- **Introduction**
- **Metamaterials**
 - Negative Refractive Index
 - Periodic and Random Material
 - Application to Enhanced Dipole Antenna
 - Application to Rotman lens
- **Metasurfaces**
 - Electromagnetic Band-Gap Surfaces
 - Wideband EBG Surfaces
 - Adaptive and Active Reflection Phase Surfaces
 - Application to Spiral Antennas
 - Application to Cognitive Radar
- **Nanotechnology**
 - Carbon Nano-Tubes
 - CNT Patches
 - Application to Gas Sensors
 - Application to Polarization-Selective Patches
- **Conclusions**



Conclusions



- **Metamaterials and metasurfaces define structures that have been known by different names in the past**
- **Metamaterial structures may lead to more efficient, smaller antennas with new features not doable with natural materials**
- **Metasurfaces provide reflection phases that can reduce antenna profiles with potential application to cognitive radar**
- **Carbon nano-tubes have high tensile-strength and light weight, with high conductivity if used in multiple layers**
- **CNTs have potential applications in body-worn electronics, sensors, and polarization selective antennas**